https://ntrs.nasa.gov/search.jsp?R=19670028731 2020-03-24T01:09:32+00:00Z

NASA TECHNICAL NOTE

NASA TN D-4194

NASA TN D-4194
c.1

LOAN COPY: RE
AFWL
KIRTLAND AFB,

TECH LIBRARY KAFB, NM
0130865

NASA TN D-4194

EFFECTS OF DIELECTRIC COVERS OVER CROSS SLOTS IN A RECTANGULAR WAVEGUIDE

by Marion C. Bailey

Langley Research Center
Langley Station, Hampton, Va.

NATIONAL AERONAUTICS AND SPACE ADMINISTRATION • WASHINGTON, D. C. • OCTOBER 1967

TECH LIBRARY KAFB, NM
0130865
NASA TN D-4194

EFFECTS OF DIELECTRIC COVERS OVER CROSS SLOTS IN A RECTANGULAR WAVEGUIDE

By Marion C. Bailey

Langley Research Center
Langley Station, Hampton, Va.

NATIONAL AERONAUTICS AND SPACE ADMINISTRATION

For sale by the Clearinghouse for Federal Scientific and Technical Information
Springfield, Virginia 22151 – CFSTI price $3.00

EFFECTS OF DIELECTRIC COVERS OVER CROSS SLOTS IN A RECTANGULAR WAVEGUIDE*

By Marion C. Bailey
Langley Research Center

SUMMARY

The purpose of this study was to determine the effects of dielectric covers upon the radiating characteristics of a cross slot in a waveguide. The slot lengths were chosen so that the data cover the waveguide bandwidth for dielectric constants from 1 to 4. Slot locations were chosen so that the far-field radiation patterns would be circularly polarized near resonance. The formulations for the general inclined slot in a waveguide coupled to free space are extended to include slots radiating into an external medium of any dielectric constant. It is also shown that plane wave theory gives a bound on the variation of power radiated for dielectric covers thicker than one-fourth wavelength. In addition to providing a simple method for obtaining circular polarization with an ablative material, this study of cross slots gives a better insight into the effects of dielectrics over the general inclined slot in the broad wall of a rectangular waveguide.

INTRODUCTION

The use of thick layers of dielectric ablative material covering the external surface of a space vehicle has been found to be an effective method of protecting the internal instrumentation from excessive heat during reentry into the earth's atmosphere at hypersonic velocities. The arraying of dielectric-covered slots in a waveguide for use as a practical reentry spacecraft antenna has been proposed by Croswell and Higgins (ref. 1) because of the inappreciable disruption in the aerodynamic streamlining of the spacecraft surface and the design flexibility of waveguide slots (ref. 2) ranging from quasi-omnidirectional (ref. 3) to narrow beamwidth and high gain (ref. 1). Croswell and Higgins investigated the effect of dielectric covers over linearly polarized shunt slots in waveguides; however, very frequently it is advantageous to be able to radiate a circularly polarized wave so that a communication link may be maintained with a linearly polarized ground-based antenna irrespective of the reentry angle of attack of the space vehicle.

*The material contained in this report was also submitted as a thesis in partial fulfillment of the requirements for the degree Master of Electrical Engineering, University of Virginia, Charlottesville, Virginia, August 1966.

Past interest in cross slots has been generally restricted to those radiating into free space (see, for example, refs. 4 and 5); however, severe changes occur in the characteristics with the addition of a dielectric cover over slots designed for free-space conditions. Because of these changes and the loss of ablation material due to heat protection requirements, an extensive knowledge of the slot characteristics as a function of the thickness and dielectric constant is required for the design of dielectric-covered cross slots for use as reentry antennas. An exact theoretical solution to this problem would require a detailed knowledge of the local reactive slot fields with and without the presence of a dielectric. Since these fields are not well-defined, the experimental approach was used and approximate theories were developed from analysis of measured results.

SYMBOLS

a	inside broad dimension of waveguide
b	inside narrow dimension of waveguide
A	amplitude of incident traveling wave
$e(\xi)$	voltage across slot
f	frequency
f_m	mean resonant frequency
f_r	average resonant frequency
g	wave scattering coefficient for general slot in waveguide
$\overline{H}$	vector magnetic field
H_o	arbitrary constant
H_x	component of magnetic field in x-direction
H_z	component of magnetic field in z-direction
$\overline{J}$	vector current density

$j = \sqrt{-1}$

$k = \frac{2\pi}{\lambda_o}$

$k_g = \frac{2\pi}{\lambda_g}$

K a complex quantity which relates modal fields to slot voltage by matching boundary conditions

l length of slot

$\bar{n}$ unit vector normal to surface of waveguide

$N = 4\sqrt{\frac{\mu_o}{\epsilon_o}}$

P_o power radiated by slot

P_i power incident upon slot from generator

r voltage reflection coefficient for single interface

t thickness of dielectric cover

TE_{10} dominant mode in rectangular waveguide

V amplitude of voltage at center of slot

w width of slot

x, z distance along X and Z axes, respectively

x_1 slot displacement measured from inside wall of waveguide to slot center

$\gamma = \frac{a}{\pi^2 bkk_g}$

ϵ relative dielectric constant

ϵ_{eq} equivalent relative dielectric constant

ϵ_o permittivity of free space

ζ complex quantity given by equation (13)

η intrinsic impedance

η_o intrinsic impedance of free space

θ angle between slot and Z-axis

λ_o free-space wavelength

$$\lambda_g = \frac{\lambda_o}{\sqrt{1 - \left(\frac{\lambda_o}{2a}\right)^2}}$$

λ_ϵ wavelength in dielectric at mean resonant frequency

λ'_ϵ wavelength in dielectric at average resonant frequency

μ relative permeability

μ_o permeability of free space

ξ direction along slot, $\frac{x}{\sin \theta}$

ρ voltage reflection coefficient for plane sheet

$|\rho|^2$ power reflection coefficient for plane sheet

ϕ angle between normal to ground plane and far-field observation point

$$\psi = \frac{2\pi t \sqrt{\epsilon}}{\lambda_o}$$

EXPERIMENT

Circular polarization may be obtained from a pair of narrow slots crossed at right angles and located at the proper point in the broad wall of a rectangular waveguide.

This fact can be explained by considering the transverse and longitudinal magnetic fields of the dominant mode (TE_{10}) in a rectangular waveguide (ref. 4).

$$H_x = H_o\sqrt{1 - \left(\frac{\lambda_o}{2a}\right)^2}\sin\left(\frac{\pi x}{a}\right) \tag{1}$$

$$H_z = -jH_o\left(\frac{\lambda_o}{2a}\right)\cos\left(\frac{\pi x}{a}\right) \tag{2}$$

Two values of x can be found for which the magnitudes of the transverse and longitudinal magnetic fields are equal. These points are given by

$$x_1 = \left(\frac{a}{\pi}\right)\cot^{-1}\left[\pm\sqrt{\left(\frac{2a}{\lambda_o}\right)^2 - 1}\right] \tag{3}$$

At points on the interior broad wall of the waveguide for which equation (3) holds, the transverse and longitudinal components of the magnetic field vector are equal in magnitude and in phase quadrature. Since the excitation voltage of a slot in a waveguide is produced by the displacement current across the slot, it follows from the boundary condition for the vector-current distribution $\overline{J} = \overline{n} \times \overline{H}$ that the excitation voltage at the center of the two narrow slots crossed at right angles would be circularly polarized at these points and radiate a circularly polarized wave, right-hand circular from one side of the waveguide center line and left-hand circular from the other, for the same direction of wave propagation inside the guide.

It was desirable for the cross slots to radiate a near circularly polarized wave at resonance. In order for the center of the cross slots to be placed at the points in the waveguide wall where the vector-current distribution is circularly polarized (eq. (3)), it would be necessary to know the resonant frequency of the dielectric-covered cross slots. An extensive study has been made of the change in the resonant length of a shunt slot in a waveguide as a function of the dielectric constant of the slot cover (ref. 1). For the purposes of this experiment, the resonant frequency of a cross slot designed to be near circularly polarized with no cover (ref. 4) was measured and the resonant length ratio determined. It was then assumed that the decrease in the resonant length of the cross slot for increasing ϵ, because of additional capacitance added to the antenna (ref. 6), would vary in the same manner as that of the shunt slot (ref. 1). This assumption is shown in figure 1 as a vertical shift in the shunt slot curve.

The experimental slots were fabricated by a process in which electrode burning is used as a means of removing the metal in the waveguide wall. The size and shape of the

electrode determines the size and shape of the slot. Figure 2 shows a typical electrode for burning cross slots in waveguides. Round-end slots 0.062 inch (0.158 cm) wide crossed at right angles in the broad wall of an RG 52/U waveguide constitute the samples used in this experiment. All dimensional tolerances were held at ±0.003 inch (0.0076 cm).

By using this design criterion, 12 slots were fabricated to be nearly circularly polarized at resonance with the appropriate dielectric cover. Different slot lengths were chosen to cover the waveguide bandwidth as shown in table I.

Figure 3 shows the geometry of the slot samples used in this study at X-band frequencies, and figure 4 shows a typical sample. The orientation of the crossed-slot pair is arbitrary, but they have been cut at $\pm 45^{\circ}$ to the Z-axis to permit longer slots to be cut without running over the side wall or waveguide center line.

The power radiated by the slot was measured as the insertion loss produced in the waveguide by the slot. The waveguide was terminated in a thermistor (voltage standing-wave ratio (VSWR) of 1.02) and a power meter was used to measure the power absorbed by the thermistor. The insertion loss due to the slot was determined by comparing these power measurements with and without the slot in the circuit. This method was permissible because of the reflectionless character of the cross slot (ref. 4). The measured VSWR was less than 1.1 for all slots considered with dielectric covers.

The four dielectric materials given in table II were investigated. Measurements were made at several discrete thicknesses to simulate the loss of material due to ablation. An attempt was made to cover the dielectric-constant range which includes many of the natural dielectrics.

EXPERIMENTAL RESULTS

The measured data for slots with no dielectric cover are presented in figure 5. Each curve represents the percent of the available power in the guide which is coupled out by the slot as a function of frequency. The resonant frequency of the slot is defined as the frequency at which maximum power is radiated by the slot, which usually occurs near a half-wavelength for free-space conditions. The free-space measurements for the 0.45-inch slots were somewhat inhibited by the excitation of a higher order mode in the waveguide whose cutoff frequency is 13.1 Gc/sec (1 Gc/sec = 1 GHz), as shown in figure 5(d); however, the resonant frequency of the slot can be established as being near 13.0 Gc/sec which is slightly below cutoff for the higher order mode.

Figure 6 shows a plot of the resonant length ratio l/λ_0 as a function of the ratio of free-space wavelength to guide wavelength λ_0/λ_g. Note the slight variation in resonant length ratio with slot displacement and also the change in resonant length with λ_0/λ_g. As will be shown later, these variations are secondary to the changes in resonant

TABLE I.- TEST SAMPLES

Sample	Slot displacement, x_1		Slot length, l		Circular polarization frequency, Gc/sec	Free-space resonant frequency, Gc/sec	Percent power radiated
	in.	cm	in.	cm			
1	0.225	0.572	0.6124	1.555	9.28	9.87	75.6
2	.211	.536	.55	1.397	9.78	10.98	63.1
3	.188	.478	.50	1.270	10.78	11.95	53.5
4	.166	.422	.45	1.143	12.02	12.95	37.6
5	.237	.602	.55	1.397	8.90	10.87	66.7
6	.204	.518	.50	1.270	10.06	11.90	55.5
7	.181	.460	.45	1.143	11.13	13.05	40.5
8	.227	.577	.55	1.397	9.22	10.92	64.8
9	.203	.516	.50	1.270	10.11	11.90	55.5
10	.178	.452	.45	1.143	11.30	13.00	40.5
11	.230	.584	.50	1.270	9.11	11.85	56.9
12	.203	.516	.45	1.143	10.11	13.02	46.0

TABLE II.- INDEX TO EXPERIMENTAL DIELECTRIC-COVERED CROSS-SLOT DATA

Dielectric constant of cover, ϵ	Loss tangent	Figure	Slot displacement, x_1		Slot length, l		Cover thickness, t		Frequency range, Gc/sec
			in.	cm	in.	cm	in.	cm	
2.0	0.0002	8(a)	0.225	0.572	0.6124	1.555	0.062 to 0.840	0.158 to 2.134	7.8 to 9.4
		8(b)	.211	.536	.55	1.397			8.8 to 10.4
		8(c)	.188	.478	.50	1.270			10.0 to 11.6
		8(d)	.166	.422	.45	1.143			11.0 to 12.4
2.57	0.0045	9(a)	0.237	0.602	0.55	1.397	0.102 to 1.015	0.259 to 2.578	8.2 to 9.8
		9(b)	.204	.518	.50	1.270			9.2 to 10.8
		9(c)	.181	.460	.45	1.143			10.4 to 12.0
2.82	0.0115	10(a)	0.227	0.577	0.55	1.397	0.122 to 0.992	0.310 to 2.520	8.0 to 9.6
		10(b)	.203	.516	.50	1.270			8.8 to 10.4
		10(c)	.178	.452	.45	1.143			10.0 to 11.6
3.76	0.0020	11(a)	0.230	0.584	0.50	1.270	0.125 to 0.882	0.318 to 2.240	8.2 to 9.8
		11(b)	.203	.516	.45	1.143			9.0 to 10.6

length due to the dielectric cover; therefore, in order to simplify the analysis, an average resonant frequency which eliminates the effects of guide wavelength and slot displacement is defined. It is suspected that for a constant ratio of slot length to slot width l/w this variation in the resonant length l/λ_o with λ_o/λ_g could be reduced; however, this effect is negligible except for very small l/w where the slot begins to look more like a round hole.

Figure 7 is a plot of the percent power coupled out of the waveguide at the slot free-space resonant frequency as a function of λ_o/λ_g. There is a slight change in radiated power due to the slot displacement since the amplitude of the waveguide modal fields which excite the slot varies across the guide. The major change, however, as indicated by the faired curve in figure 7, depends upon the length of the slot. This decrease in

radiated power with increase in resonant frequency, or increase in λ_o/λ_g, is expected since the length of the slot, or the size of the aperture, is becoming smaller at resonance. Note that for the trivial case as λ_o/λ_g approaches unity or as the resonant frequency approaches infinity, the slot disappears and no power would be coupled out of the waveguide.

The measured data for the dielectric-covered cross slots are presented in figures 8 to 11 where the dielectric constant ϵ is the main differentiating parameter. The data are presented in the form of a series of curves for each slot length and dielectric constant. Each series of curves consists of a plot of the percent of the power coupled out of the waveguide by the slot as a function of frequency for various dielectric cover thicknesses. An index to these data is given in table II. Note that the slots still maintain a resonant behavior when covered by a dielectric layer; however, the resonance curves are more broadened, especially for the shorter slot lengths and larger dielectric constants, because of the added capacitance.

ANALYSIS OF RESULTS

Change in Resonant Length

A study of the measured data reveals that the addition of a dielectric cover over a cross slot causes a significant change in the resonant frequency (the frequency at peak radiated power). It was also noted from figures 8 to 11 that the resonant frequency depends upon the thickness of the dielectric cover. This variation in resonant frequency as a function of the cover thickness is presented in figure 12. The resonant frequency decreases very rapidly with the addition of a dielectric cover up to a thickness of approximately $0.2\lambda_\epsilon$. The resonant frequency has a sinusoidal variation with a period of $t \approx 0.5\lambda_\epsilon$ for thicknesses greater than $0.2\lambda_\epsilon$.

In order to analyze the effect of the dielectric cover upon the radiation characteristics of the cross slots, it was necessary to define an average resonant frequency f_r which is only a function of the slot length and the dielectric constant. This was accomplished by determining the mean resonant frequency f_m for each slot sample from the curves of figure 12 in the region where the resonant frequency was periodic as a function of dielectric thickness. Then, by using this mean resonant frequency f_m and the slot length l, a value of resonant length ratio l/λ_o was calculated for each slot sample. All values of l/λ_o related to a particular dielectric constant were averaged to eliminate the secondary effects of guide wavelength and slot displacements from the data.

As an example of the averaging process, consider the case of $\epsilon = 2.0$. The mean resonant frequencies f_m for slot lengths l of 0.6124, 0.55, 0.50, and 0.45 inch were determined from the curves of figure 12 as the frequencies about which the curves oscillated for thicknesses greater than about $0.2\lambda_\epsilon$. These frequencies were 8.64, 9.67, 10.52,

and 11.78 Gc/sec corresponding to resonant lengths l/λ_o of 0.448, 0.450, 0.445, and 0.449. The numerical average of 0.448 was then defined as the average resonant length for $\epsilon = 2.0$ and the frequency which would give an l/λ_o of 0.448 was defined as the average resonant frequency f_r.

With this process, an average l/λ_o was obtained for each dielectric constant; then, the plot shown in figure 13 was constructed. The maximum deviations of the measured resonant frequencies of figure 12 from the average l/λ_o for dielectric thicknesses greater than $0.2\lambda_e$ are indicated by the vertical lines in figure 13. With a knowledge of the dielectric constant ϵ and the slot length l, an average resonant frequency f_r can be determined from the plot shown in figure 13. The vertical dashed lines in figures 8 to 11 indicate the appropriate defined average resonant frequency f_r.

A first attempt at approximating the change in resonant length with the addition of a dielectric cover might be to assume that the space surrounding the slot is completely filled with a material of dielectric constant ϵ. Then the resonant length would be given by

$$\frac{l}{\lambda_o} = \frac{(l/\lambda_o)_o}{\sqrt{\epsilon}} \tag{4}$$

where $(l/\lambda_o)_o$ is the resonant length with no cover and l/λ_o is the resonant length with a dielectric cover. However, as shown in figure 14, equation (4) predicts too short a resonant length; thus, the slot can be considered equivalently filled with a dielectric constant less than ϵ. Then the resonant length as a function of the dielectric constant of the cover would be

$$\frac{l}{\lambda_o} = \frac{(l/\lambda_o)_o}{\sqrt{\epsilon_{eq}}} \tag{5}$$

where ϵ_{eq} would be determined from the empirical curve of figure 14.

Power Radiated as a Function of Cover Thickness

One characteristic of primary interest is the variation in power radiated as a function of cover thickness. By using the definition of average resonant frequency f_r values were obtained from the measured data curves of figures 8 to 11 and presented in figures 15 to 18 as percent power radiated by the slot as a function of the dielectric thickness in wavelengths t/λ'_ϵ. It was noted that these curves became sinusoidal with a period of $t \approx 0.5\lambda'_\epsilon$ for thicknesses greater than $0.2\lambda'_\epsilon$. This condition suggested that the local slot fields probably extend only into very thin layers of dielectric material and plane wave theory may be applicable for dielectric covers thicker than about $0.2\lambda'_\epsilon$. The

power reflection coefficient for a plane wave normally incident upon a plane lossless dielectric sheet is given in reference 7 (p. 32-5) by

$$|\rho|^2 = \frac{4r^2\sin^2\psi}{(1 - r^2)^2 + 4r^2\sin^2\psi} \tag{6}$$

where

$$r = \frac{1 - \sqrt{\epsilon}}{1 + \sqrt{\epsilon}}$$

and

$$\psi = \frac{2\pi t\sqrt{\epsilon}}{\lambda_o}$$

The power reflection coefficient alternates through maxima and minima as a function of thickness or frequency. Maximum reflection occurs at odd multiples of the quarter-wavelength thickness. These extreme values are given by

$$|\rho|^2_{min} = 0 \tag{7}$$

$$|\rho|^2_{max} = \left(\frac{2r}{1 + r^2}\right)^2 \tag{8}$$

In order to relate equations (7) and (8) to the curves in figures 15 to 18, it was assumed that the point $t \approx 0.6\lambda'_\epsilon$ (where maximum power radiated occurs) corresponds to the case of no reflections as given by equation (7). For the case of maximum reflections as predicted by equation (8), the amount of power coupled out of the slot at $t \approx 0.6\lambda'_\epsilon$ is reduced by $|\rho|^2_{max}$. The horizontal dashed lines in figures 15 to 18 are the bounds on the variation of power radiated by the slot as a function of dielectric thickness. These bounds appear to give a useful prediction of power variations for dielectric thicknesses greater than about $0.2\lambda'_\epsilon$. It must be remembered, however, that the upper bound was chosen as the maximum measured value at $t \approx 0.6\lambda'_\epsilon$.

SLOTS RADIATING INTO SEMI-INFINITE MEDIUM

Stevenson (ref. 8) and Watson (ref. 9) have solved the problem of the general inclined-displaced slot radiating into free space by treating the slot as an obstacle in the waveguide and relating the scattered waves in the waveguide to an assumed voltage across the slot. The purpose of this section is to show that this free-space theory can be

extended to slots radiating into a semi-infinite medium which is different from that inside the waveguide. The special case of the cross slot is used for a comparison with experimental data, but the extension of the theory is applicable to the general inclined-displaced slot in the rectangular waveguide.

Extension of Free-Space Theory

If a wave of complex amplitude A inside the waveguide is incident upon the slot from the left, there will be waves scattered to the right and left inside the waveguide of amplitudes $-gA$ and $g'A$, respectively. These wave scattering coefficients, g and g', are given by Watson (ref. 9) as

$$\left.\begin{aligned} g &= -\frac{\gamma|\zeta|^2}{K} \\ g' &= \frac{\gamma\zeta^2}{K} \end{aligned}\right\} \tag{9}$$

where*

$$\gamma = \frac{a}{\pi^2 bkk_g}$$

and, as usual, $k = 2\pi/\lambda_o$ and $k_g = 2\pi/\lambda_g$.

The complex quantities ζ and K relate the amplitude of the assumed field in the slot to the amplitude of the modal fields in the waveguide. If the voltage across the slot is assumed to be of the form

$$e(\xi) = V \cos k\xi \tag{10}$$

where ξ denotes the direction along the slot, by reference 9 (eq. 66.1)

$$\frac{V}{A} = \frac{\zeta}{K} \tag{11}$$

in the notation of this paper.

In the process of matching boundary conditions at the slot, Stevenson (ref. 8) and Watson (ref. 9) found that for a half-wavelength slot, the quantity ζ is given by

$$\zeta = \int_{-\lambda_o/4}^{\lambda_o/4} f(\xi)\cos k\xi \, d\xi \tag{12}$$

*The author feels that there is a misprint in Watson's expression for this parameter which has been confirmed by Maxum (ref. 2).

where $\frac{Af(\xi)}{\mu_o}$ is the ξ-component, along the slot, of the tangential magnetic field due to the incident TE_{10} traveling wave of amplitude A. For the slot in the broad wall of the rectangular waveguide

$$\zeta = \frac{\pi^2}{ka^2}\cos\theta\left[I(\theta)\cos\left(\frac{\pi x_1}{a}\right) - jJ(\theta)\sin\left(\frac{\pi x_1}{a}\right)\right] + \frac{\pi k_g}{ka}\sin\theta\left[J(\theta)\cos\left(\frac{\pi x_1}{a}\right) - jI(\theta)\sin\left(\frac{\pi x_1}{a}\right)\right] \tag{13}$$

where

$$I(\theta) = \frac{\cos\left(\frac{p\pi}{2}\right)}{1 - p^2} + \frac{\cos\left(q\,\frac{\pi}{2}\right)}{1 - q^2}$$

$$J(\theta) = \frac{\cos\left(\frac{p\pi}{2}\right)}{1 - p^2} - \frac{\cos\left(q\,\frac{\pi}{2}\right)}{1 - q^2}$$

$$p = \frac{k_g}{k}\cos\theta - \frac{\pi}{ka}\sin\theta$$

$$q = \frac{k_g}{k}\cos\theta + \frac{\pi}{ka}\sin\theta$$

where θ is the inclination of the slot with respect to the Z-axis and x_1 is the displacement of the slot center from the inside wall of the waveguide.

The complete calculation of K is a complicated matter which involves a doubly infinite series; however, for resonant slots, K is usually assumed to be real (ref. 9). The real part of K can be determined very easily by consideration of the following equation of energy taken from Watson (ref. 9) for an incident wave of unit amplitude

$$\frac{1}{N\gamma}\left(1 - |g'|^2\right) = \frac{|1 - g|^2}{N\gamma} + \frac{|V|^2}{N_o} \tag{14}$$

where N and N_o are normalizing factors which depend upon the system of units employed. The factor N also depends upon the field vector, and Watson defines his magnetic Hertz-vector such that in MKS units

$$N = 4\sqrt{\frac{\mu_o}{\epsilon_o}} = 4(120\pi) \tag{15}$$

and

$$N_o = \frac{\eta_o^2}{73} \tag{16}$$

where η_o is the intrinsic impedance of free space.

The last term on the right-hand side of equation (14) corresponds to the radiation from a thin half-wavelength slot in an infinite conducting plane with an excitation voltage of amplitude V at its center. If it is assumed that the slot voltage still maintains a cosine distribution at resonance with the external medium, the intrinsic impedance of free space in equation (16) can be replaced by the intrinsic impedance of the medium outside the waveguide

$$\eta = \sqrt{\frac{\mu\mu_o}{\epsilon\epsilon_o}} \tag{17}$$

where μ and ϵ are the relative permeability and permittivity of the semi-infinite medium outside. If μ and ϵ are assumed to be real, equation (14) can now be written in a somewhat more general form

$$\frac{1}{N\gamma}\left(1 - |g'|^2\right) = \frac{1}{N\gamma}\left(1 - 2\mathrm{Re}(g) + |g|^2\right) + \frac{|V|^2}{N_o \frac{\mu}{\epsilon}} \tag{18}$$

where $\mathrm{Re}(g)$ means the real part of g.

Solving for $\mathrm{Re}(g)$ from equation (18) and using equations (9), (11), (15), and (16) yields

$$\mathrm{Re}(g) = \frac{\gamma^2|\zeta|^4}{|K|^2} + \frac{\epsilon(73)\gamma|\zeta|^2}{60\pi\mu|K|^2} \tag{19}$$

Also from equation (9)

$$\mathrm{Re}(g) = -\gamma|\zeta|^2\mathrm{Re}\left(\frac{1}{K}\right) \tag{20}$$

Therefore, equating the right-hand sides of equations (19) and (20) and using the fact that

$$\mathrm{Re}\left(\frac{1}{K}\right) = \frac{\mathrm{Re}(K)}{|K|^2} \tag{21}$$

yields explicitly

$$\mathrm{Re}(K) = -\gamma|\zeta|^2 - \frac{\epsilon(73)}{60\pi\mu} \tag{22}$$

Since it was assumed that K is real when the slot is resonant, by substituting $\mathrm{Re}(K)$ for K in equation (9), g is given by

$$g = \frac{1}{1 + \dfrac{\epsilon(73)}{60\pi\mu\gamma|\zeta|^2}} \tag{23}$$

Equation (23) still holds for resonant slots radiating into the semi-infinite medium defined by μ and ϵ whether the slot is located in the broad or the narrow face of the waveguide; however, for the slot in the narrow face ζ is given by a different expression, which can be obtained by integration of the field over the slot as indicated in equation (12).

An expression similar to equation (23) could also be obtained for g', but for the special case of the cross slot according to Simmons (ref. 4), the backward scattered waves from the two legs at $\pm 45^{\circ}$, treated separately, are equal in magnitude but opposite in phase, and thereby cancel each other. This reflectionless property was also observed for cross slots covered with a dielectric sheet. Because of this reflectionless property of the cross slot, the relative power radiated by the cross slot at resonance is easily calculated as

$$\frac{P_o}{P_i} = 1 - |1 - 2g|^2 \tag{24}$$

where P_o is the power radiated by the slot, P_i is the power from the generator propagated down the waveguide, and g is the scattering due to one leg of the cross slot and is given in equation (23).

Comparison With Measurements On Cross Slots Under Finite Dielectric Slabs

Equation (24) is plotted in figure 19 along with the measured values of maximum radiated power from figures 15 to 18 at a dielectric thickness of $t \approx 0.6\lambda_\epsilon'$ for comparison. The values of g for each experimental slot were calculated from equation (23) at the defined average resonant frequency f_r. For these calculations it was assumed that the relative permeability μ was unity and the relative permittivity or dielectric constant ϵ was purely real. For the materials used in this experiment, these assumptions are very good.

Notice from figure 19 that the measured values of relative power radiated for dielectric constants greater than unity at a thickness of $t \approx 0.6\lambda_\epsilon'$ are about 1 dB lower than that predicted by equation (24). There is good agreement between theory and measurement for the slots with no dielectric cover ($\epsilon = 1.0$); therefore, one might suspect

that the internal fields of the waveguide are further disturbed by the dielectric sheet over the slot. In addition, because of the broad beamwidth of the slot element pattern, a considerable amount of energy could be trapped in the dielectric material, and thereby introduce surface waves propagating along the sheet. These waves are partially reflected from the edges of the finite width sheet and coupled back into the waveguide; thus, the measured power radiated by the slot is reduced. Evidence of the existence of these surface waves can be observed in the far-field radiation patterns.

RADIATION PATTERNS

The far-field radiation pattern for a typical cross slot with no dielectric sheet is shown in figure 20 and the radiation patterns for the same slot with various dielectric thicknesses are shown in figure 21. The slot was located at the center of a 12- (30.48 cm) by 22-inch (55.88 cm) ground plane and the patterns were measured in the plane which includes the long dimension. However, the edge effect still perturbs the pattern for one polarization more than for the other, and thus causes the ellipticity ratio to vary over the main beam of the pattern. This edge effect of the finite-size ground plane is seen in figure 20, for no dielectric cover, as a broadening of the beam as well as periodic fluctuations when the electric field is polarized parallel to the plane of incidence (horizontal). As observed in figure 21, these fluctuations in the horizontal polarization tend to be amplified when a dielectric sheet is placed over the slot; and, in addition, fluctuations are introduced into the vertical polarized pattern because of the unpolarized radiation from the scattering of the surface waves at the edges of the dielectric sheet. Verification of the fact that there is indeed energy being radiated from the edges is indicated by the agreement between the periodicity of the ripples and the periodicity of two point-source radiators located 11 inches apart and radiating with equal phase.

The on-axis ellipticity ratio (at $\phi = 0^{o}$) for this particular slot was about 1 dB for no dielectric cover. The ellipticity ratio (at $\phi = 0^{o}$) varied with the thickness of the dielectric sheet with a maximum deviation from circular of about 5 dB. One observation that can be made from this limited set of patterns is that the ellipticity ratio tends to vary in the same manner as the power radiated as a function of dielectric thickness. The best ellipticity ratio occurs in the neighborhood of $t \approx 0.6\lambda_{\epsilon}$ and the worst deviations from circular polarization tend to occur approximately $0.25\lambda_{\epsilon}$ on either side of this thickness. No particular significance has been applied to this observation as yet, because of the very limited patterns available, but it is mentioned as a possible starting point for a more extensive study of the effects of dielectric thickness upon the ellipticity ratio.

CONCLUDING REMARKS

The primary purpose of this experiment was to determine the design parameters of dielectric-covered cross slots as a circularly polarized flush-mounted antenna for possible use in atmospheric reentry applications. It was found that the power radiated by the cross slot as well as its resonant frequency varied in a sinusoidal manner with changes in dielectric thickness. The power radiated and resonant frequency are also a function of the dielectric constant. Theories are presented for the general resonant slot in a rectangular waveguide covered by a semi-infinite medium; these theories give mean power predictions within 20-percent accuracy when applied to cross slots covered by a finite dielectric slab.

It was found that an appreciable amount of energy is trapped inside the dielectric sheet, and thereby introduces surface wave modes which complicate the design problem. The ellipticity ratio, as well as the measured power radiated by the slot, is greatly affected by these surface waves and the finite-size ground plane. The on-axis ellipticity varied from 1 to 5 dB with changes in dielectric thickness. Future work in this area should include a detailed analysis of the surface wave effects.

Langley Research Center,
National Aeronautics and Space Administration,
Langley Station, Hampton, Va., March 10, 1967,
125-22-02-02-23.

REFERENCES

1. Croswell, William F.; and Higgins, Robert B.: Effects of Dielectric Covers Over Shunt Slots in a Waveguide. NASA TN D-2518, 1964.

2. Maxum, Bernard J.: Resonant Slots With Independent Control of Amplitude and Phase. IRE Trans. Antennas and Propagation, vol. AP-8, no. 4, July 1960, pp. 384-389.

3. Cockrell, C. R.; and Croswell, W. F.: The Application of Circular Arrays to Spacecraft Antenna Problems. Presented at Electronics Systems Symposium of International Conference and Exhibit on Aerospace Electro-Technology, Apr. 1964.

4. Simmons, Alan J.: Circularly Polarized Slot Radiators. IRE, Trans. Antennas Propagation, vol. AP-5, no. 1, Jan. 1957, pp. 31-36.

5. Getsinger, W. J.: Elliptically Polarized Leaky-Wave Array. IRE Trans. Antennas and Propagation, vol. AP-10, no. 2, Mar. 1962, pp. 165-171.

6. Compton, R. T., Jr.: The Admittance of Aperture Antennas Radiating Into Lossy Media. Rept. 1691-5 (NASA Grant No. NsG-448), Antenna Lab., Ohio State Univ. Res. Found., Mar. 15, 1964.

7. Kay, Alan F.: Radomes and Absorbers. Antenna Engineering Handbook, Henry Jasik, ed., McGraw-Hill Book Co., Inc., 1961, pp. 32-1 – 32-40.

8. Stevenson, A. F.: Theory of Slots in Rectangular Wave-Guides. J. Appl. Phys., vol. 19, no. 1, Jan. 1948, pp. 24-38.

9. Watson, W. H.: The Physical Principles of Wave Guide Transmission and Antenna Systems. Clarendon Press (Oxford), 1947.

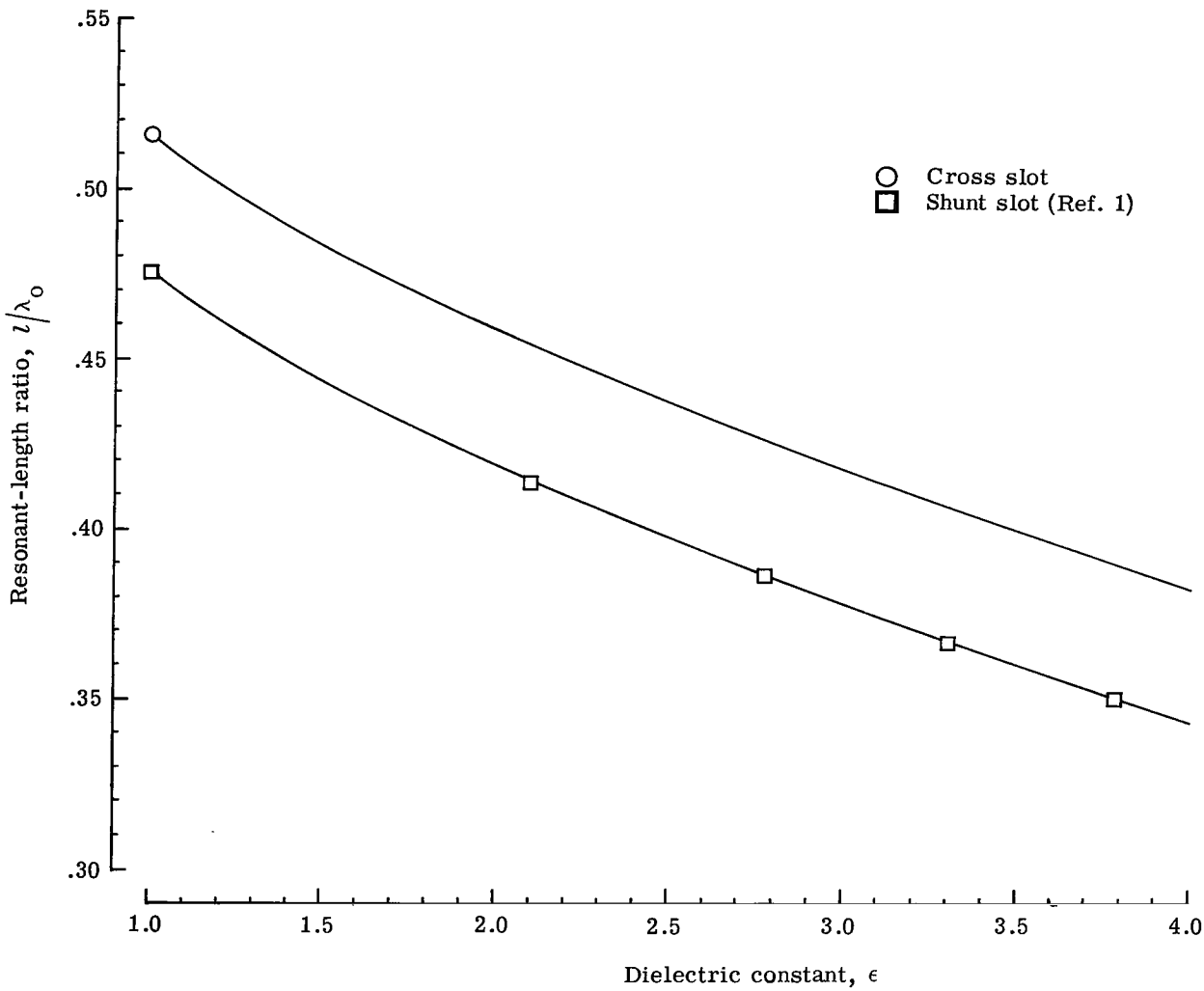

Figure 1.- Resonant-length ratio as a function of dielectric constant.

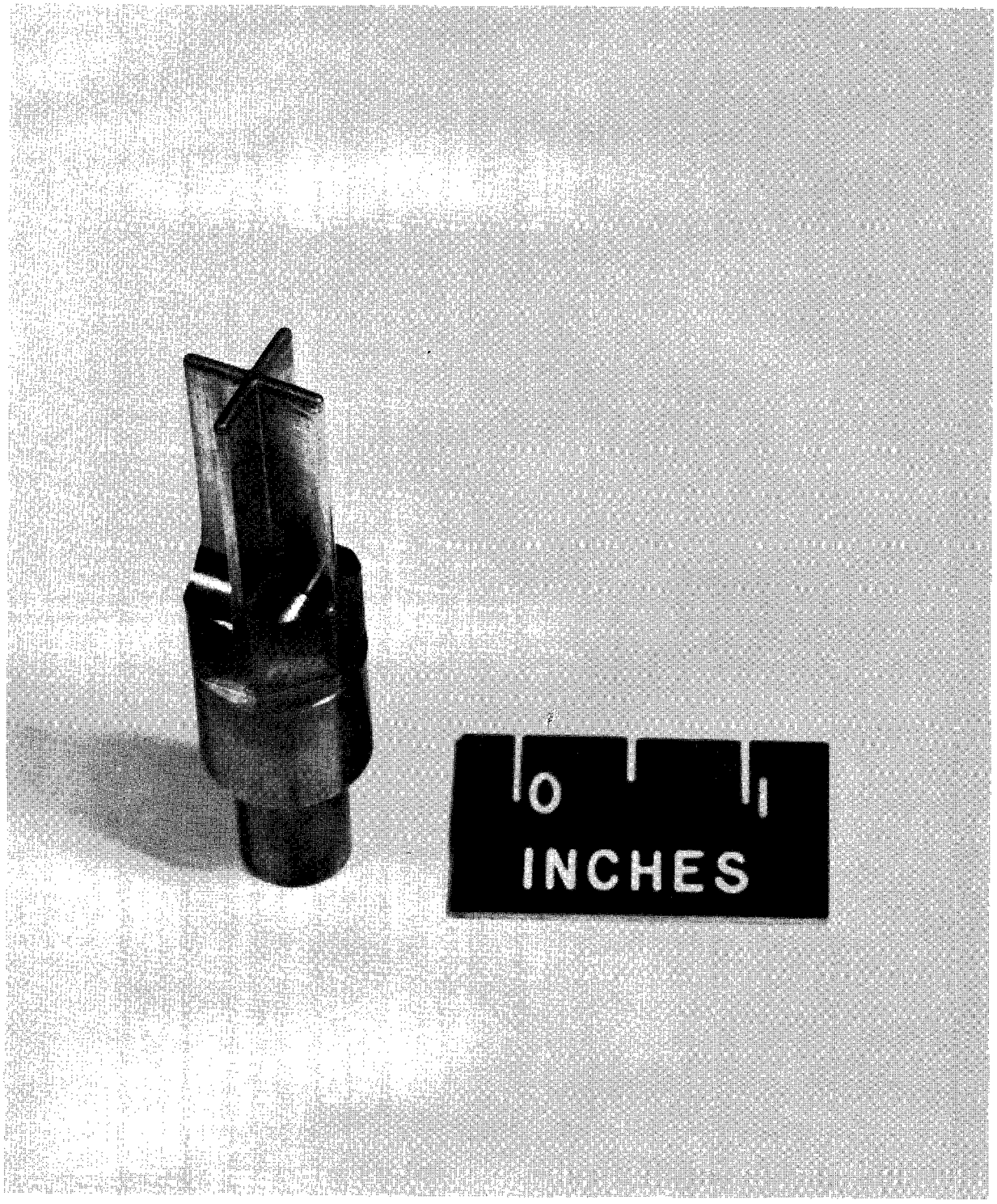

Figure 2.- Electrode for burning cross slots in waveguides. L-66-5470

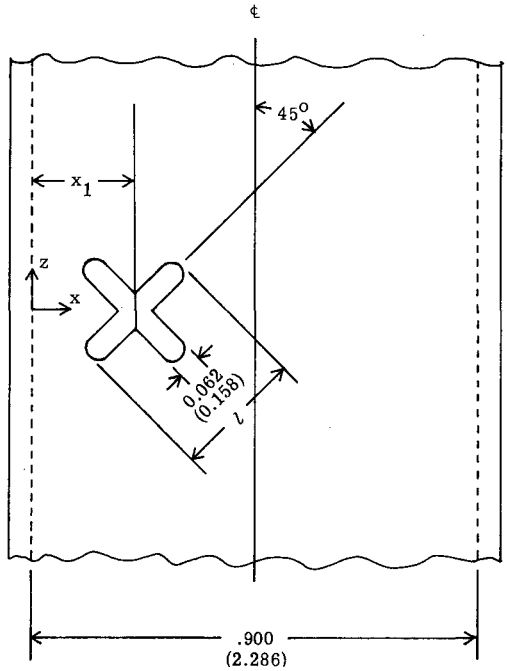

Figure 3.- Cross slot geometry. Linear dimensions are in inches (centimeters).

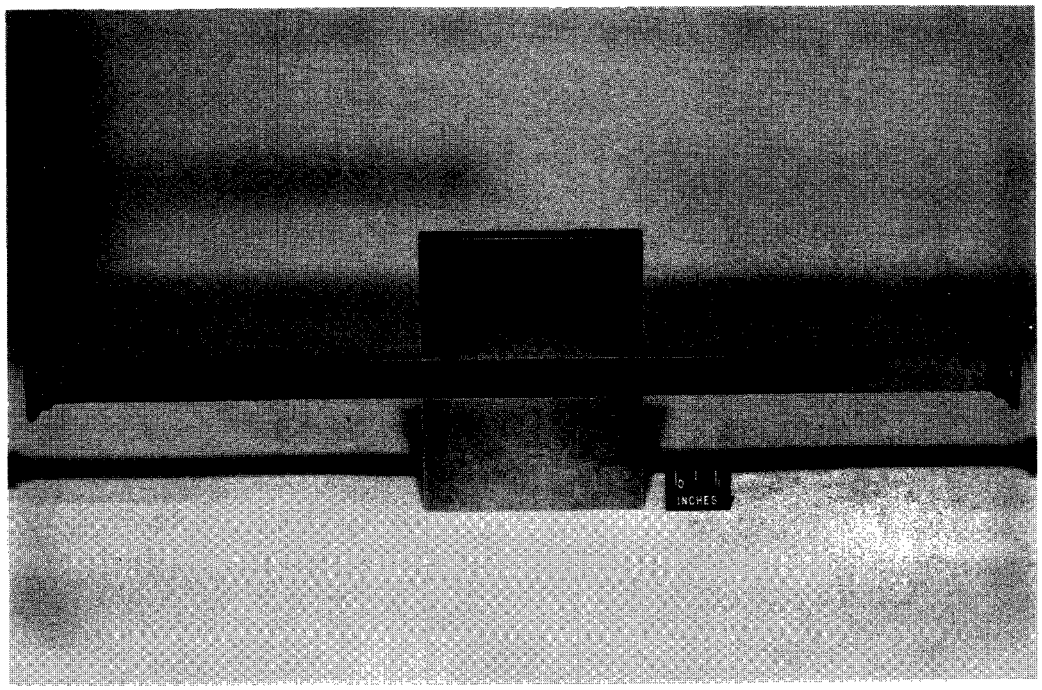

Figure 4.- Typical cross slot sample. L-67-1062

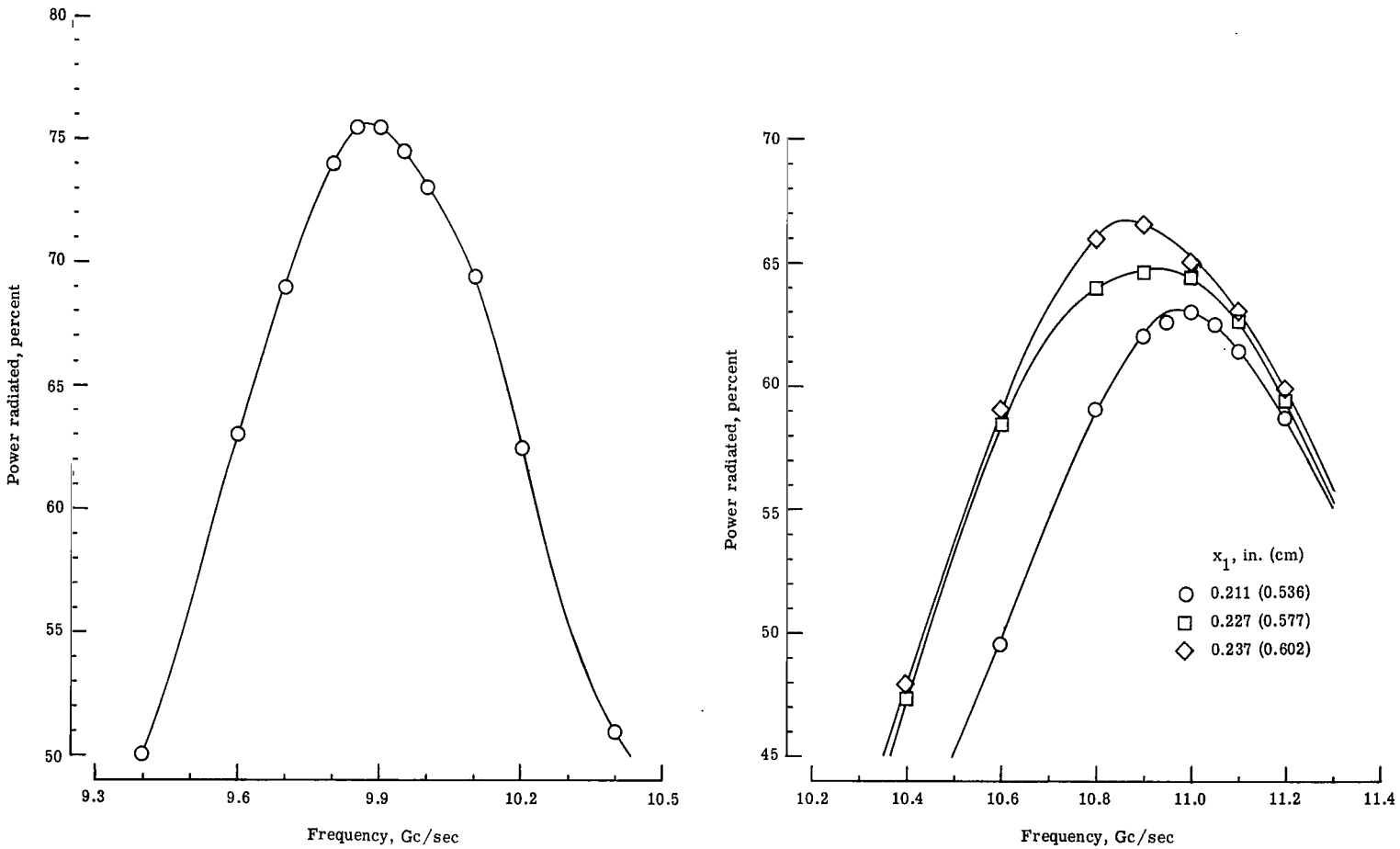

(a) l = 0.6124 inch (1.555 cm); x_1 = 0.225 inch (0.572 cm).

(b) l = 0.55 inch (1.397 cm).

Figure 5.- Measured power coupled out of waveguide by cross slots with no dielectric cover.

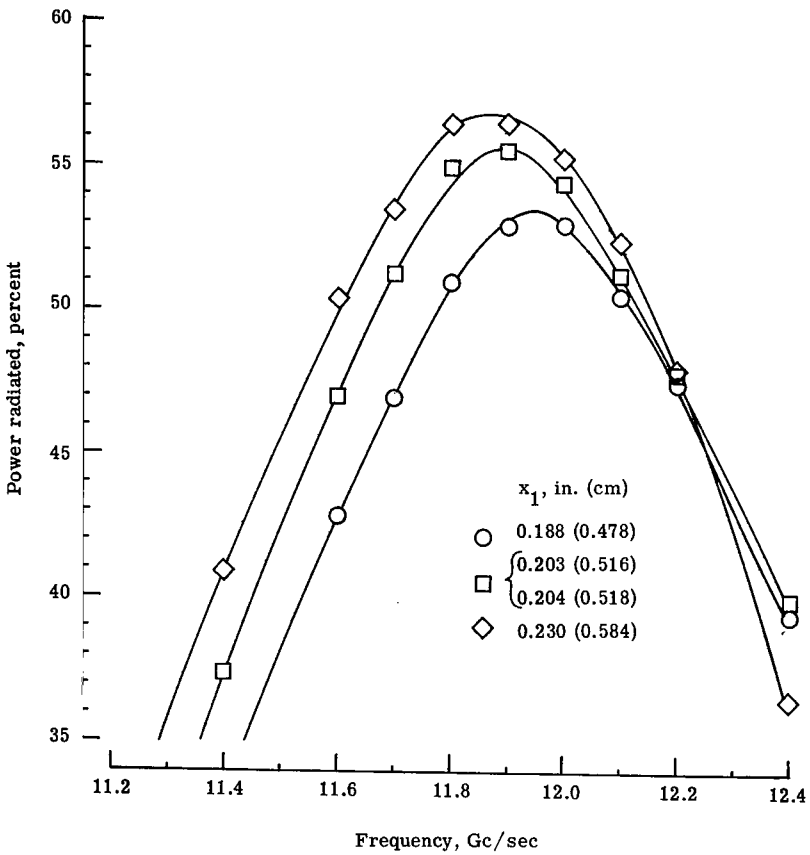

(c) l = 0.50 inch (1.270 cm).

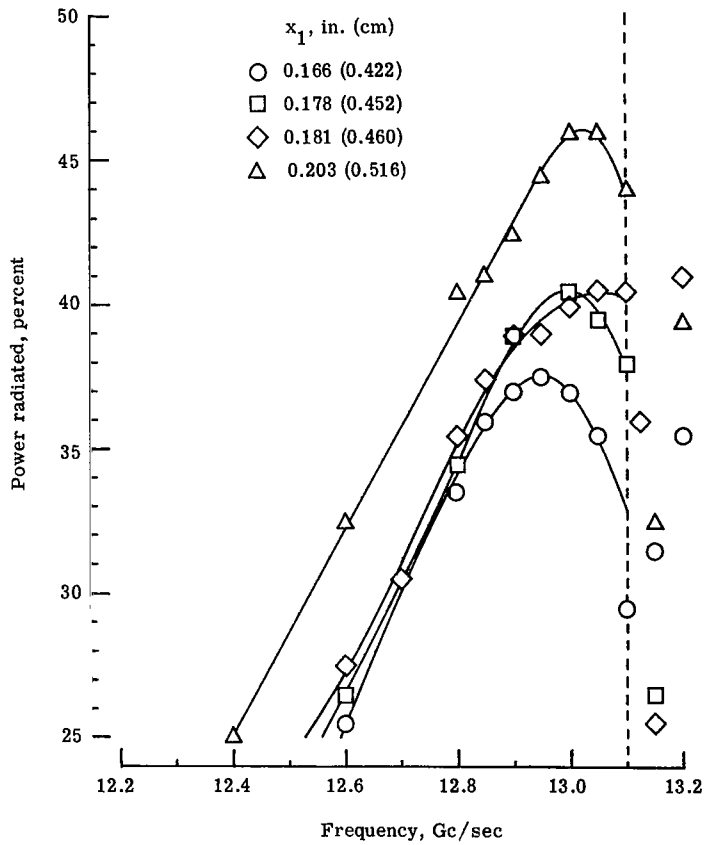

(d) l = 0.45 inch (1.143 cm).

Figure 5.- Concluded.

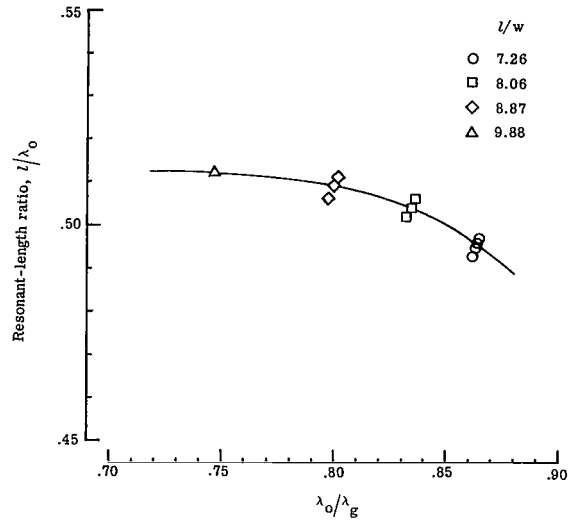

Figure 6.- Resonant-length ratio of cross slots with no cover as a function of λ_o/λ_g.

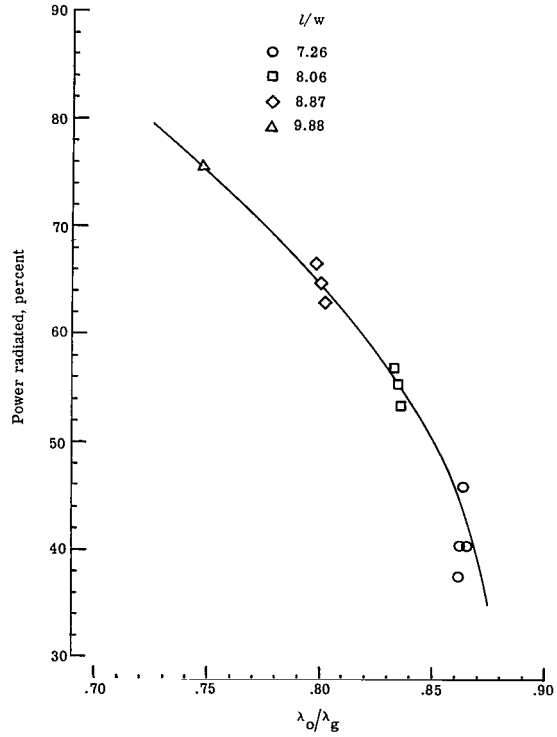

Figure 7.- Measured power radiated as a function λ_o/λ_g for cross slots at resonance with no cover.

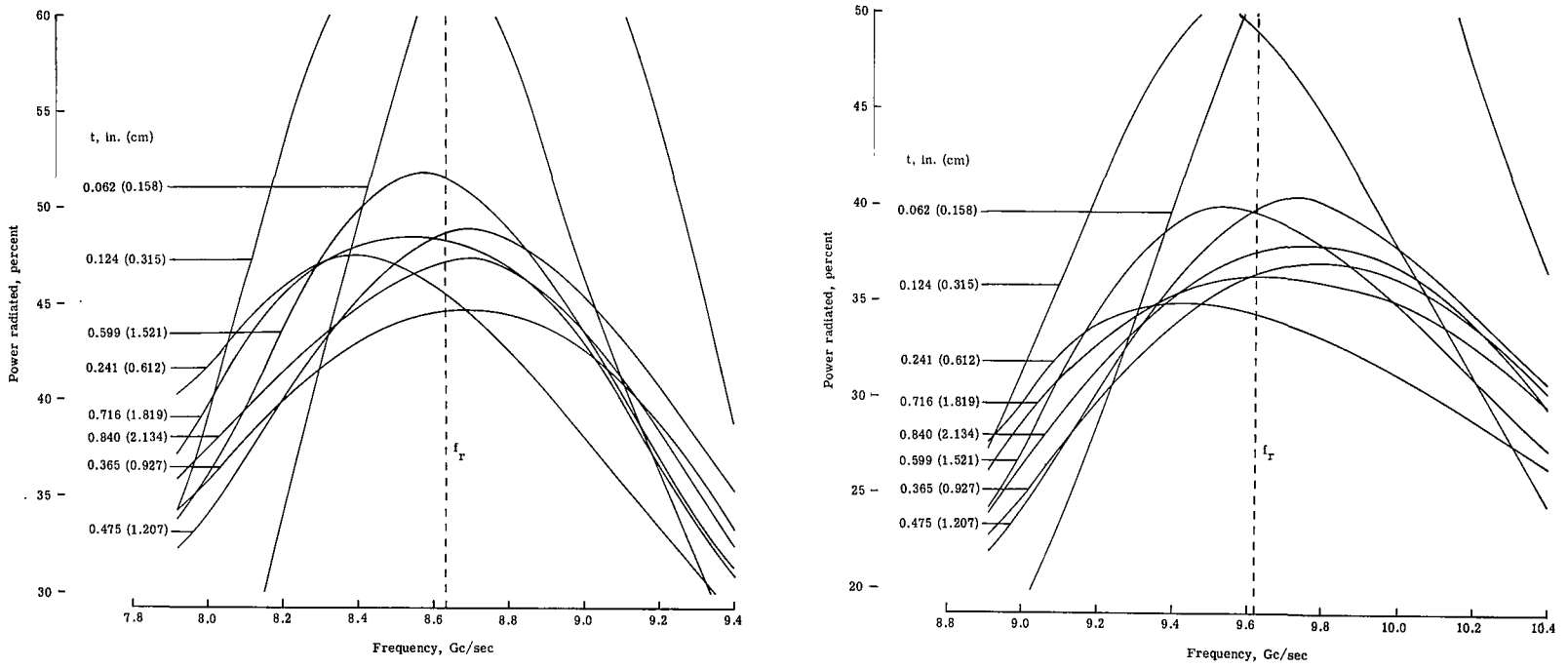

(a) l = 0.6124 inch (1.555 cm); x_1 = 0.225 inch (0.572 cm). (b) l = 0.55 inch (1.397 cm); x_1 = 0.211 inch (0.572 cm).

Figure 8.- Measured power radiated by a cross slot as a function of frequency for various cover thicknesses. ϵ = 2.00.

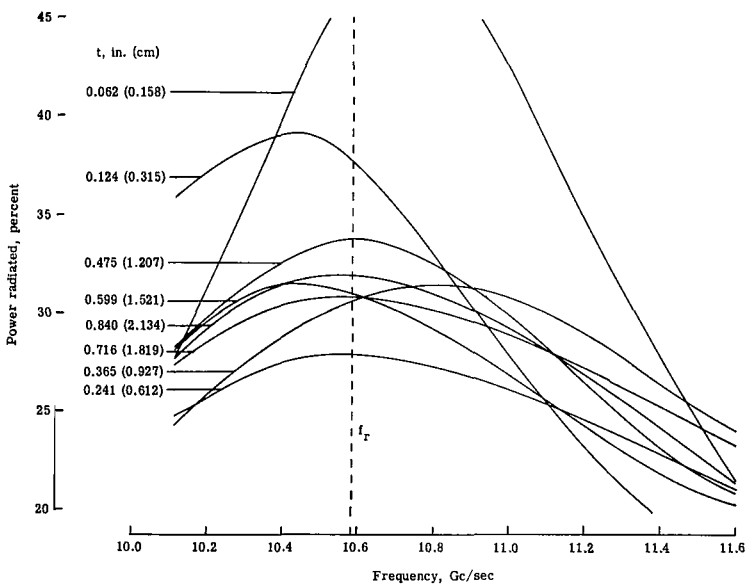

(c) l = 0.50 inch (1.270 cm); x_1 = 0.188 inch (0.478 cm).

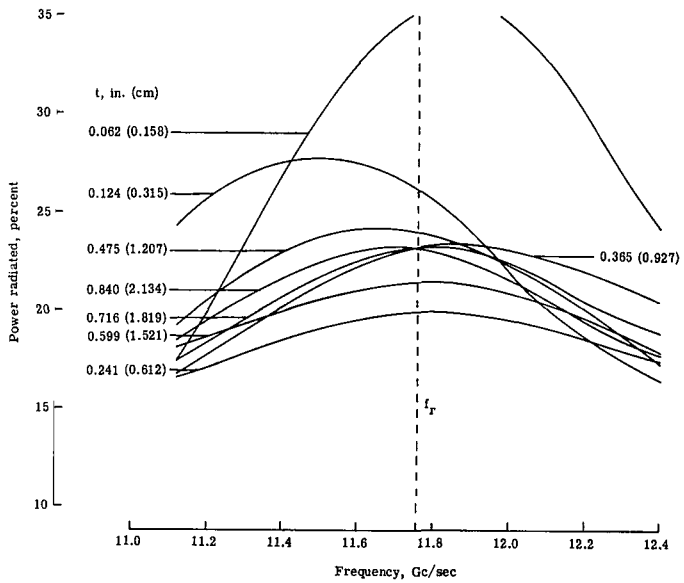

(d) l = 0.45 inch (1.143 cm); x_1 = 0.166 inch (0.422 cm).

Figure 8.- Concluded.

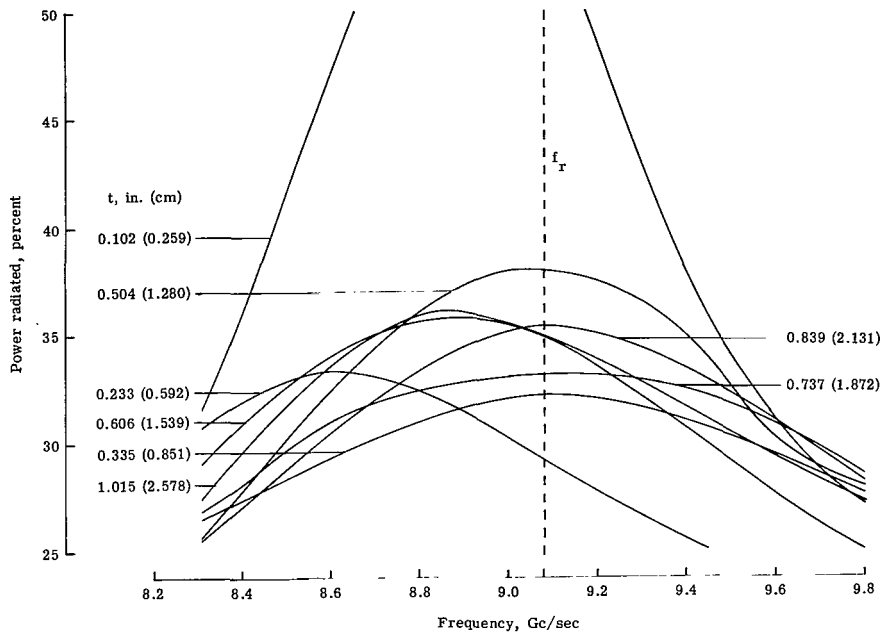

(a) ℓ = 0.55 inch (1.397 cm); x_1 = 0.237 inch (0.602 cm).

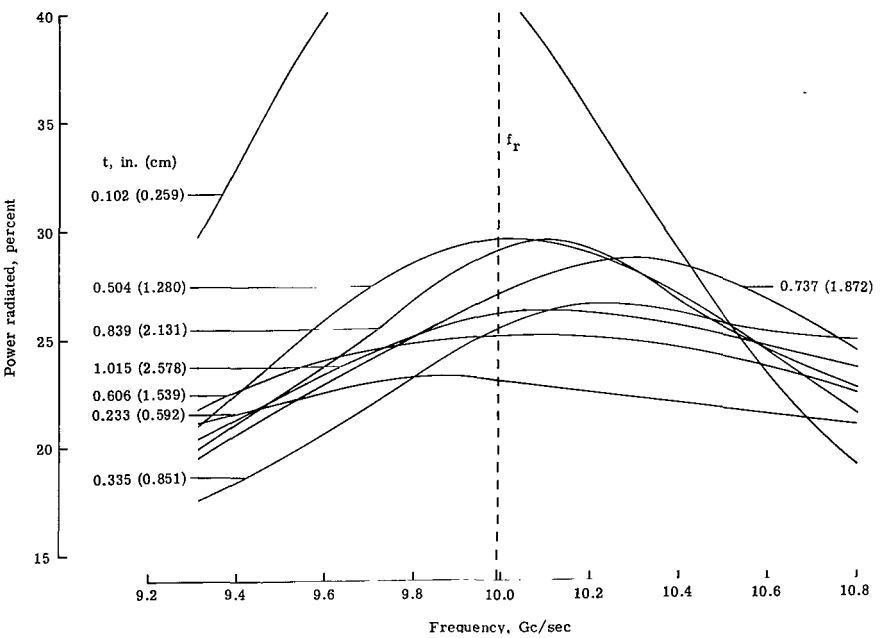

(b) ℓ = 0.50 inch (1.270 cm); x_1 = 0.204 inch (0.518 cm).

Figure 9.- Measured power radiated by a cross slot as a function of frequency for various cover thicknesses. ε = 2.57.

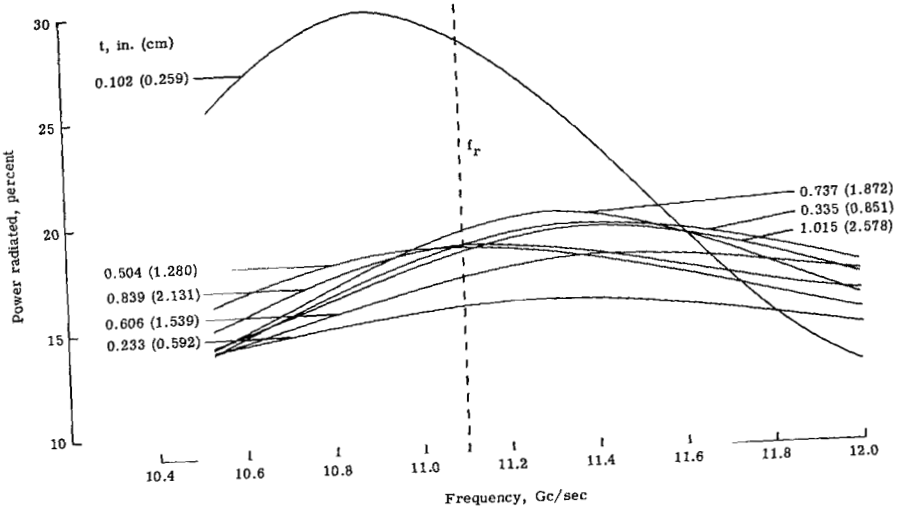

(c) ℓ = 0.45 inch (1.143 cm); x_1 = 0.181 inch (0.460 cm).

Figure 9.- Concluded.

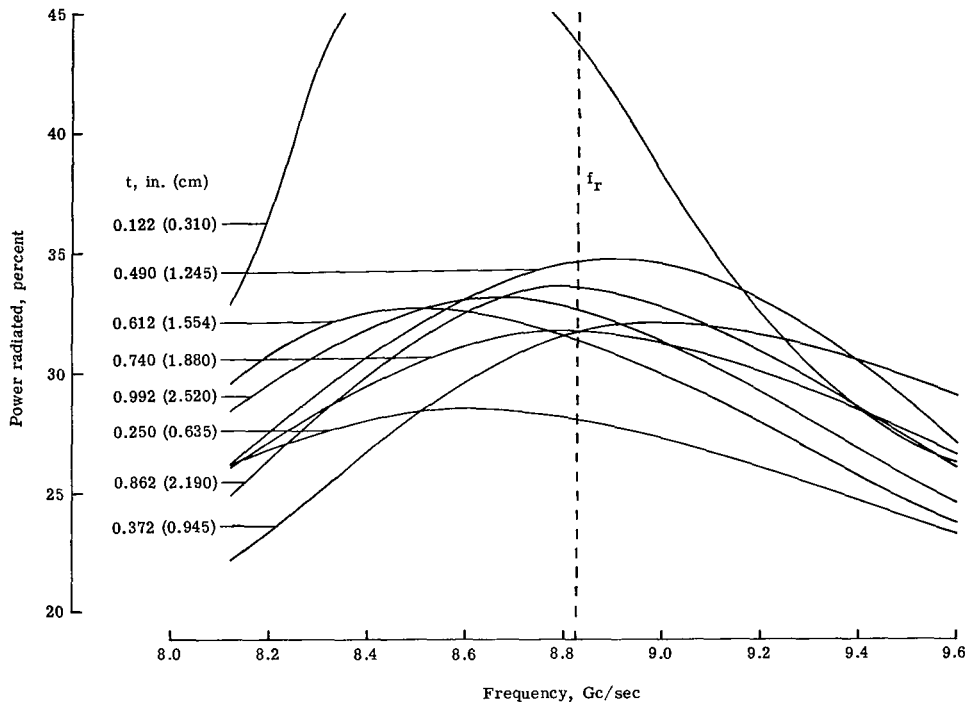

(a) ℓ = 0.55 inch (1.397 cm); x_1 = 0.227 inch (0.577 cm).

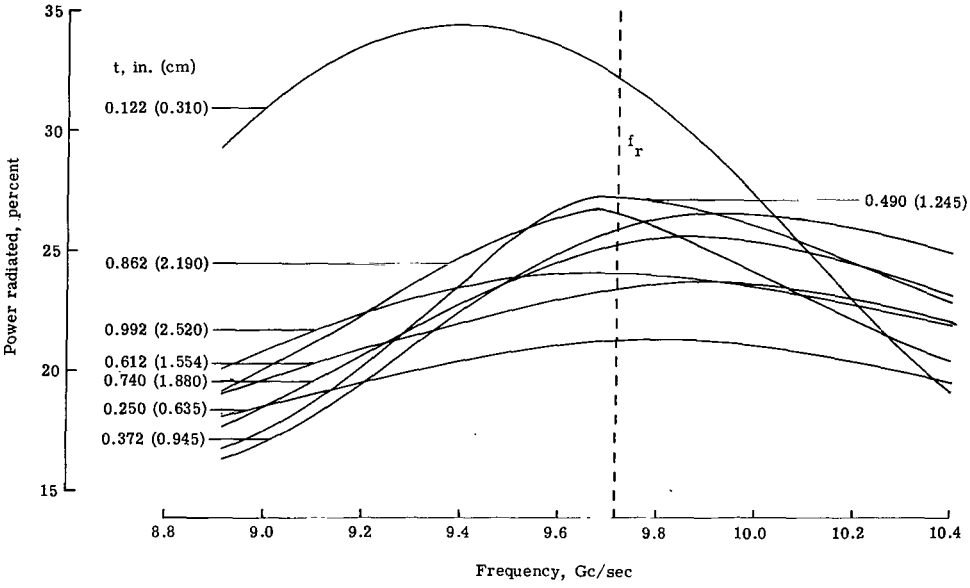

(b) ℓ = 0.50 inch (1.270 cm); x_1 = 0.203 inch (0.516 cm).

Figure 10.- Measured power radiated by a cross slot as a function of frequency for various cover thicknesses. ε = 2.82.

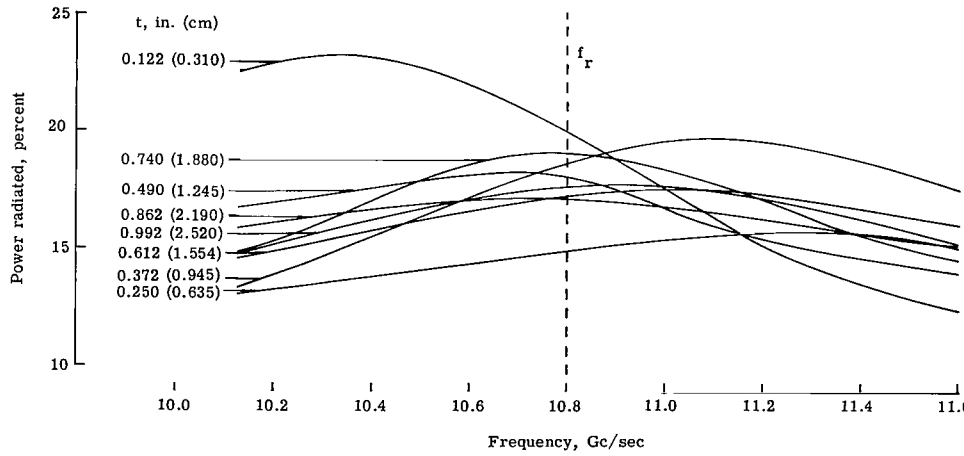

(c) l = 0.45 inch (1.143 cm); x_1 = 0.178 inch (0.452 cm).

Figure 10.- Concluded.

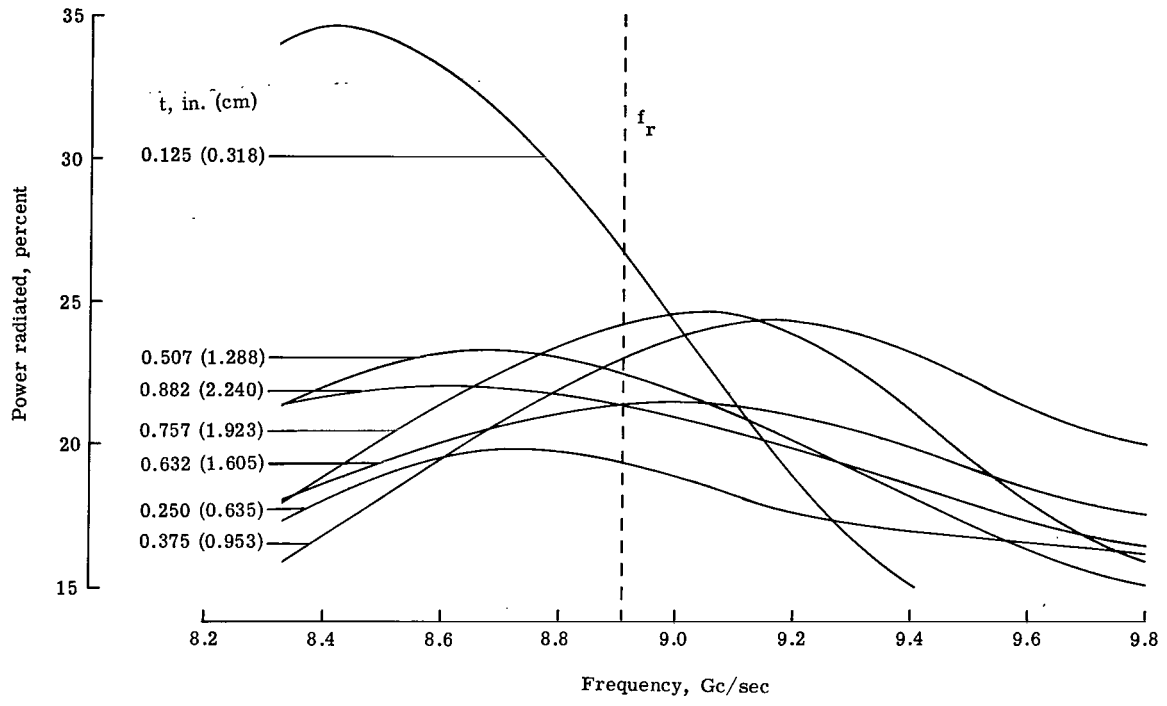

(a) l = 0.50 inch (1.270 cm); x_1 = 0.230 inch (0.584 cm).

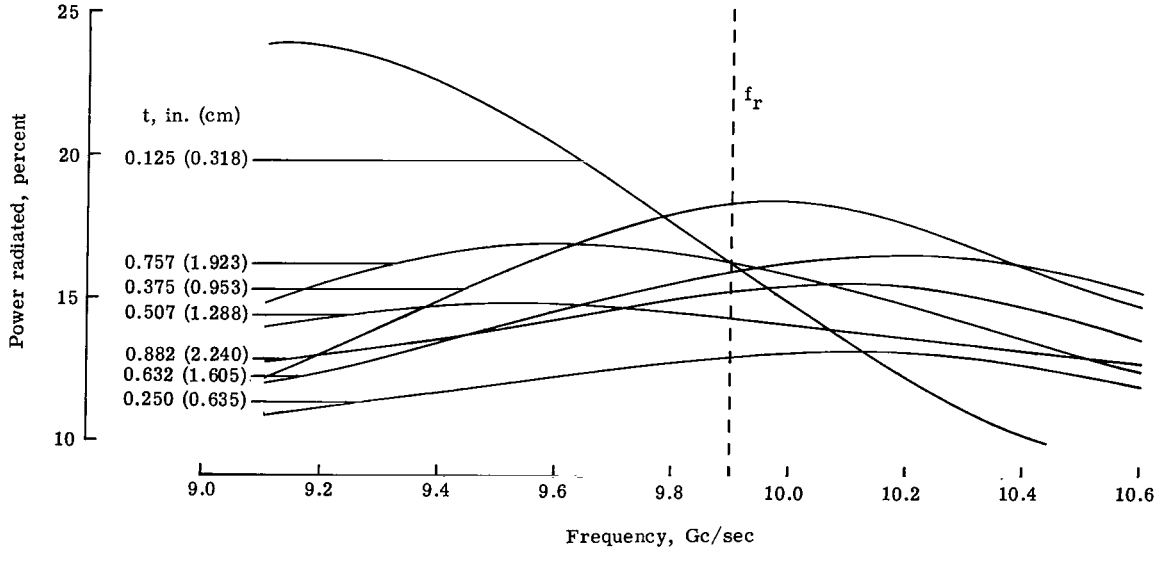

(b) l = 0.45 inch (1.143 cm); x_1 = 0.203 inch (0.516 cm).

Figure 11.- Measured power radiated by a cross slot as a function of frequency for various cover thicknesses. ε = 3.76.

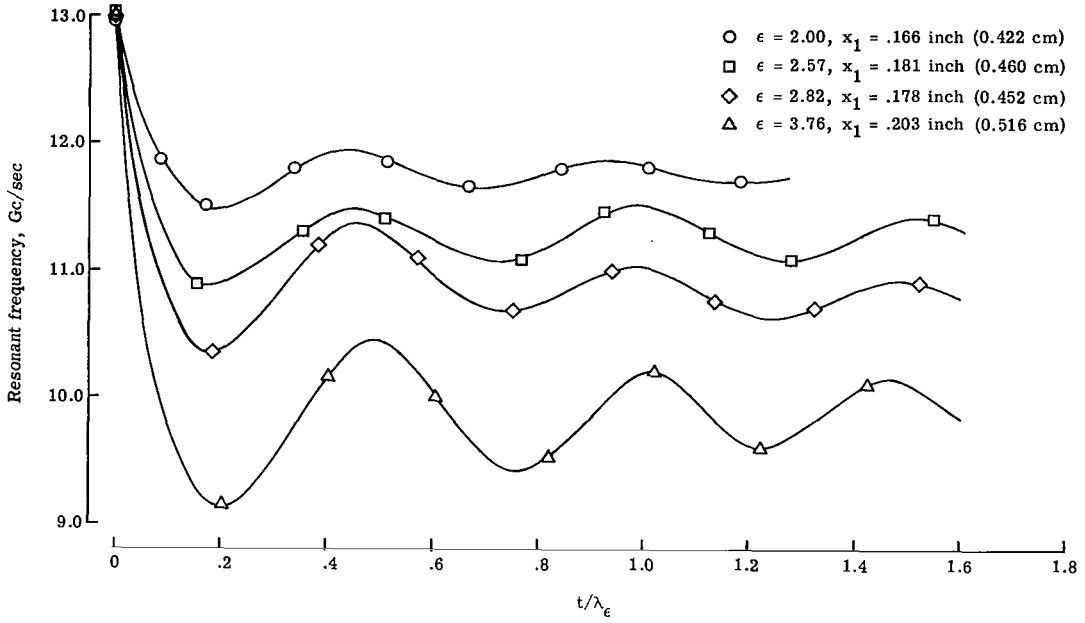

(a) l = 0.45 inch (1.143 cm).

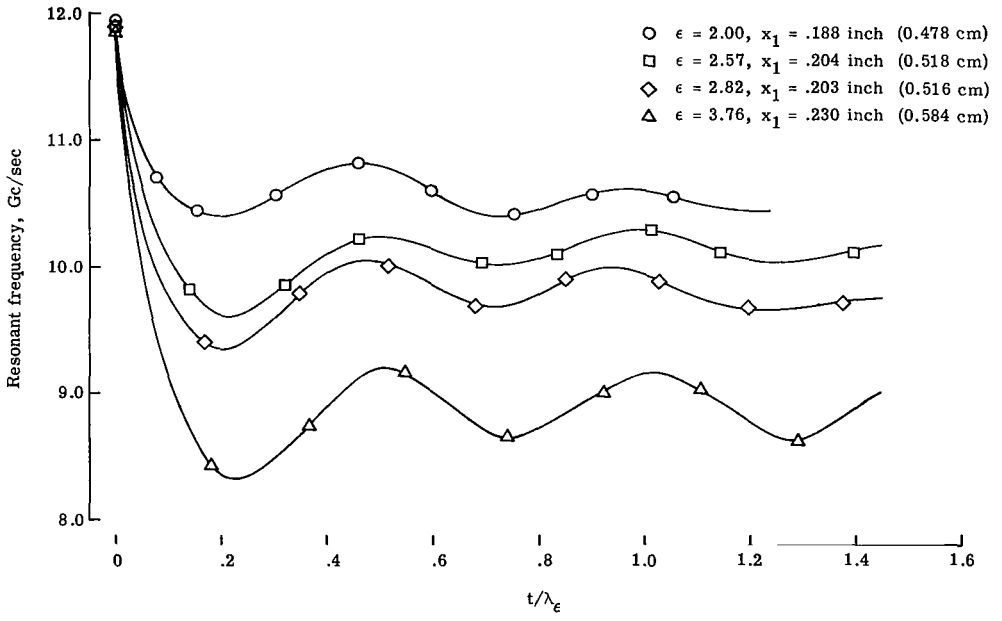

(b) l = 0.50 inch (1.270 cm).

Figure 12.- Resonant frequency of cross slot as a function of cover thickness for various dielectric covers.

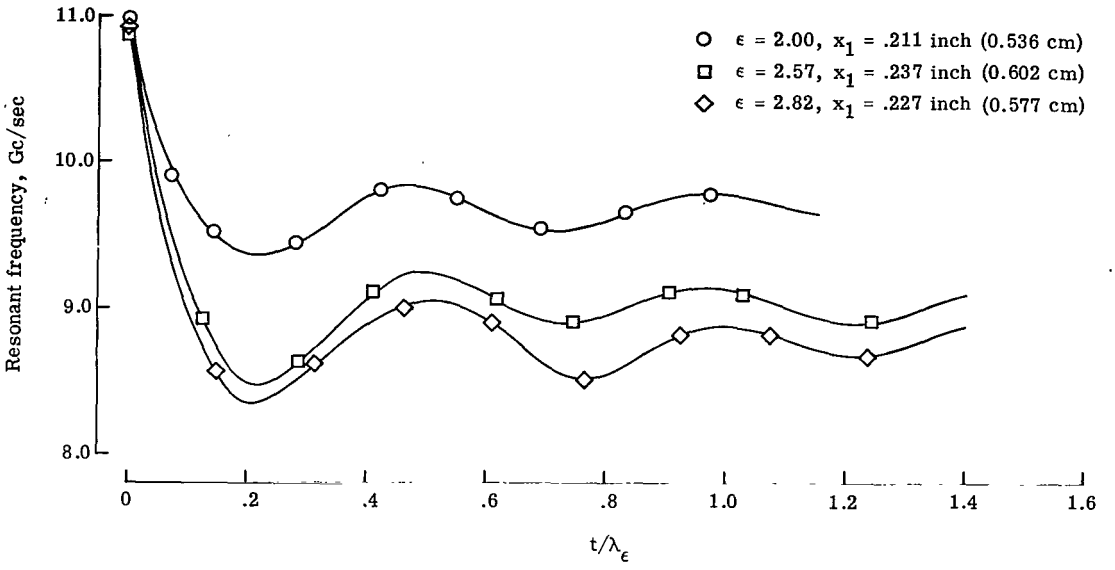

(c) l = 0.55 inch (1.397 cm).

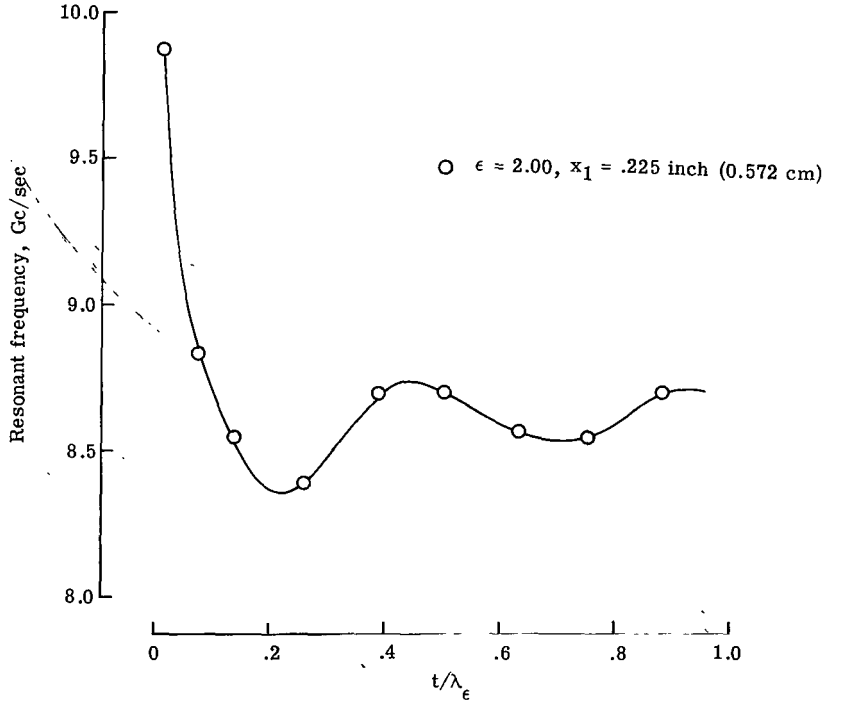

(d) l = 0.6124 inch (1.555 cm).

Figure 12.- Concluded.

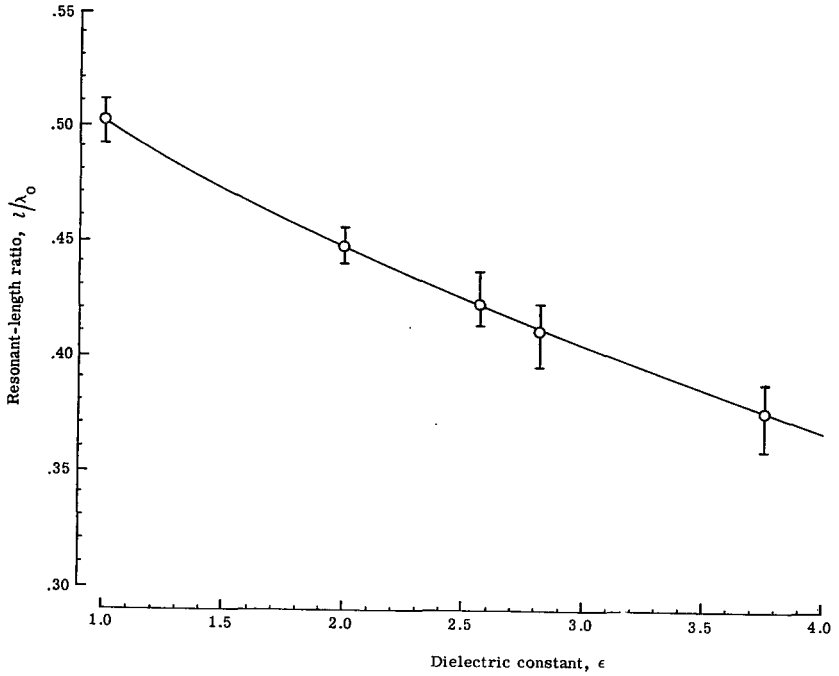

Figure 13.- Average resonant-length ratio of cross slots as a function of dielectric constant.

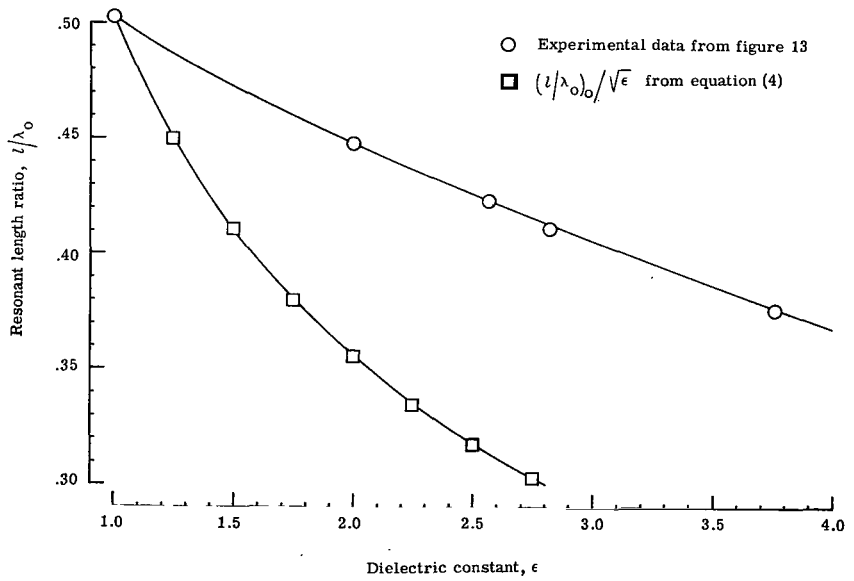

Figure 14.- Comparison between measured and calculated resonant length of cross slots.

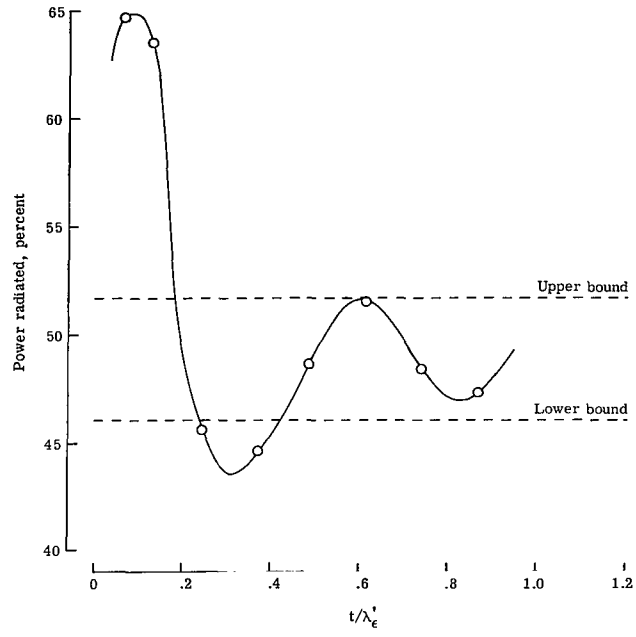

(a) f_r = 8.64 Gc/sec; l = 0.6124 inch (1.555 cm); x_1 = 0.225 inch (0.572 cm).

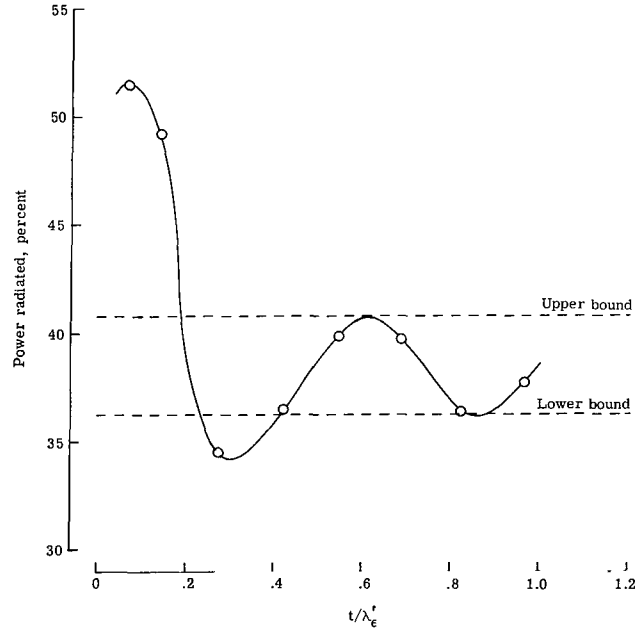

(b) f_r = 9.62 Gc/sec; l = 0.55 inch (1.397 cm); x_1 = 0.211 inch (0.536 cm).

Figure 15.- Measured power radiated by a cross slot at the average resonant frequency as a function of the cover thicknesses. ϵ = 2.00.

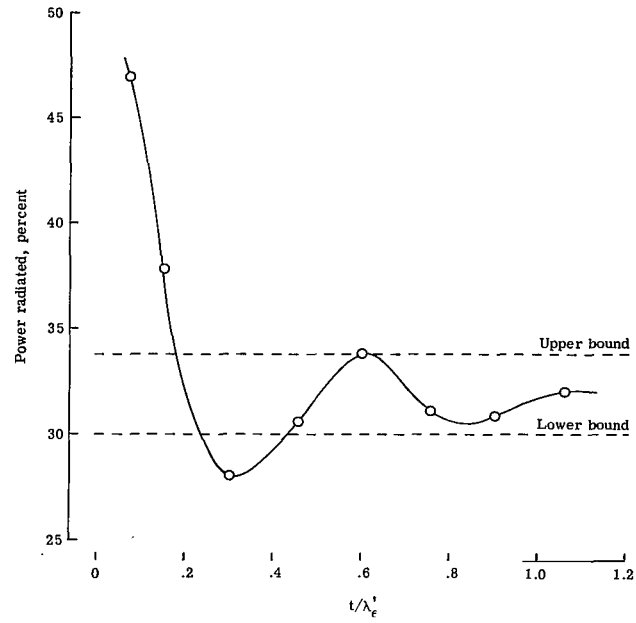

(c) f_r = 10.59 Gc/sec; l = 0.50 inch (1.270 cm); x_1 = 0.188 inch (0.478 cm).

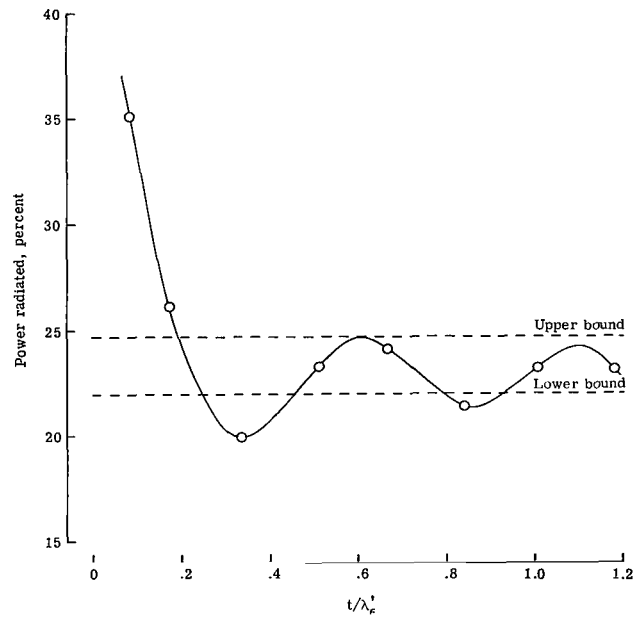

(d) f_r = 11.76 Gc/sec; l = 0.45 inch (1.143 cm); x_1 = 0.166 inch (0.422 cm).

Figure 15.- Concluded.

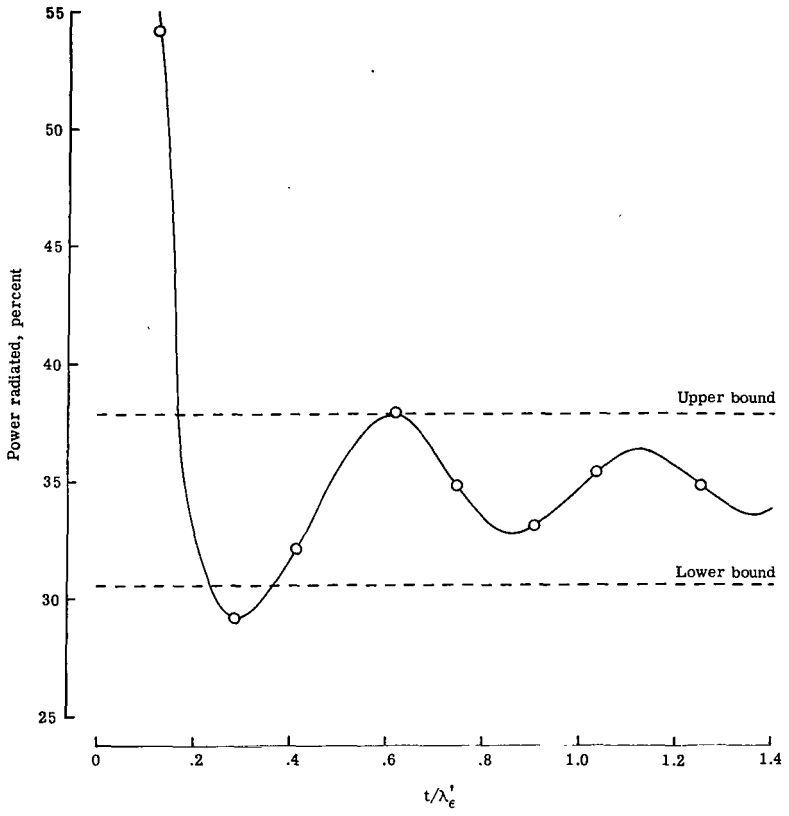

(a) f_r = 9.08 Gc/sec; l = 0.55 inch (1.397 cm); x_1 = 0.237 inch (0.602 cm).

Figure 16.- Measured power radiated by a cross slot at the average resonant frequency as a function of the cover thickness. ϵ = 2.57.

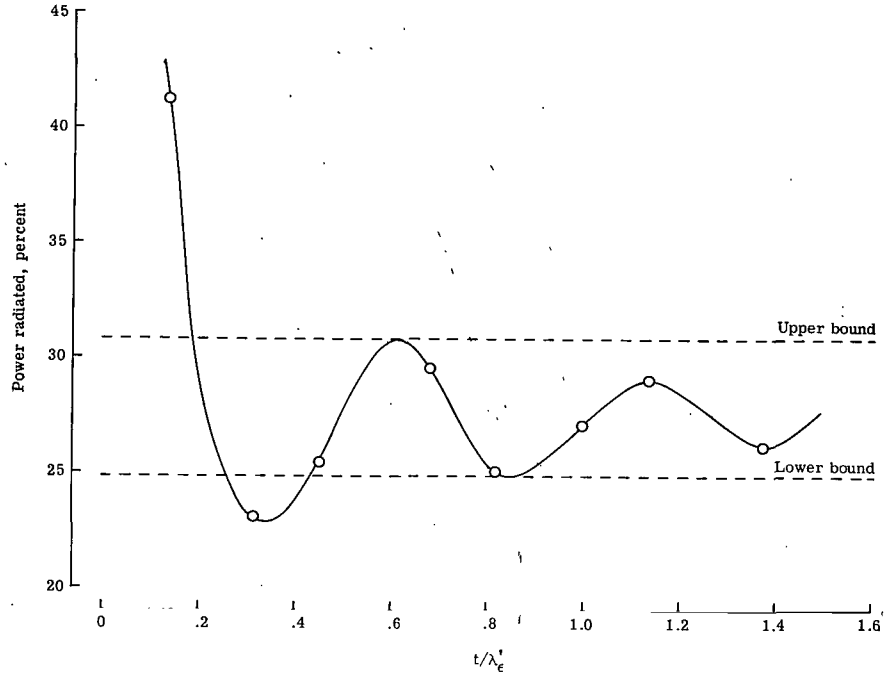

(b) f_r = 9.99 Gc/sec; l = 0.50 inch (1.270 cm); x_1 = 0.204 inch (0.518 cm).

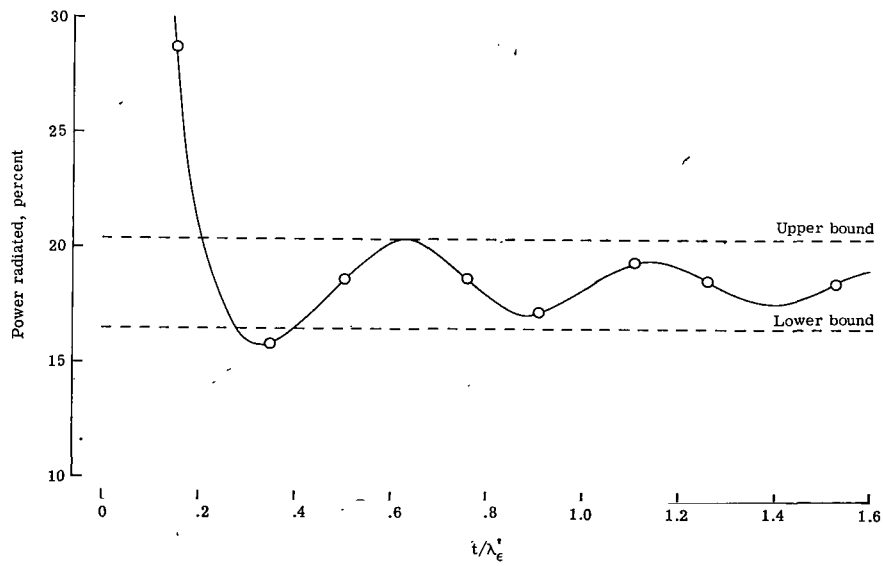

(c) f_r = 11.10 Gc/sec; l = 0.45 inch (1.143 cm); x_1 = 0.181 inch (0.460 cm).

Figure 16.- Concluded.

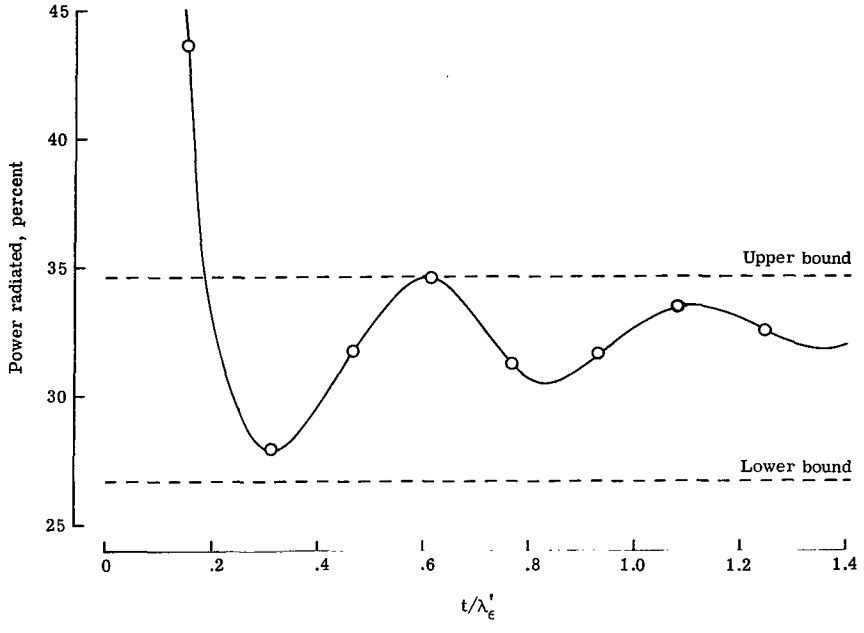

(a) f_r = 8.83 Gc/sec; l = 0.55 inch (1.397 cm); x_1 = 0.277 inch (0.577 cm).

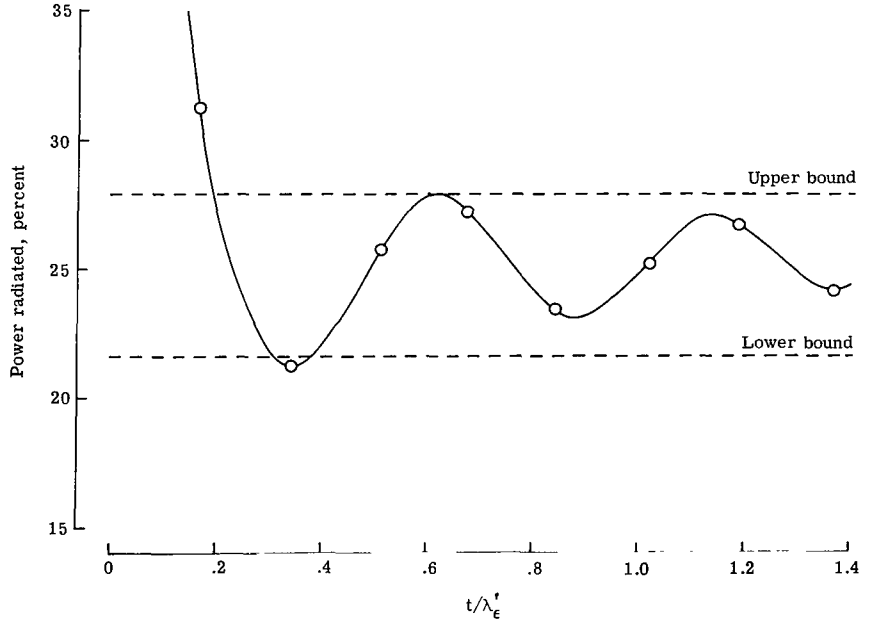

(b) f_r = 9.72 Gc/sec; l = 0.50 inch (1.270 cm); x_1 = 0.203 inch (0.516 cm).

Figure 17.- Measured power radiated by a cross slot at average resonant frequency as a function of cover thickness. ε = 2.82.

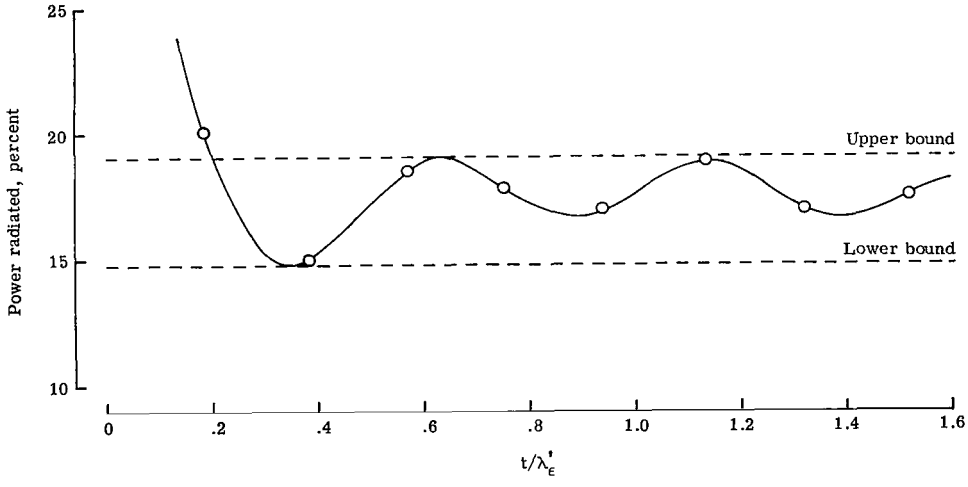

(c) f_r = 10.80 Gc/sec; l = 0.45 inch (1.143 cm);
x_1 = 0.178 inch (0.452 cm).

Figure 17.- Concluded.

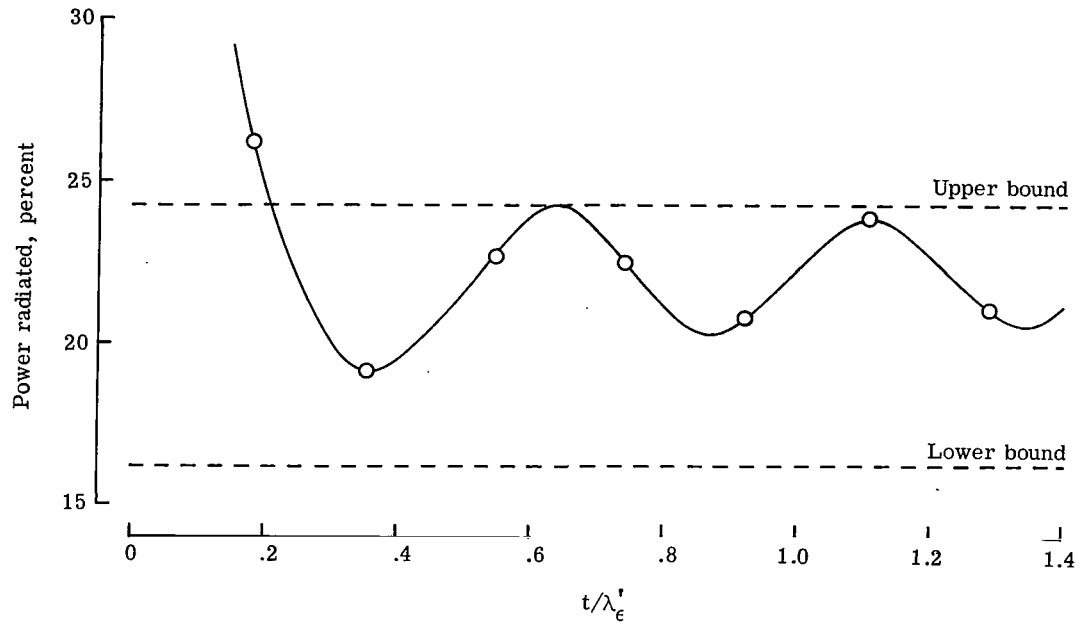

(a) f_r = 8.91 Gc/sec; l = 0.50 inch (1.270 cm); x_1 = 0.230 inch (0.584 cm).

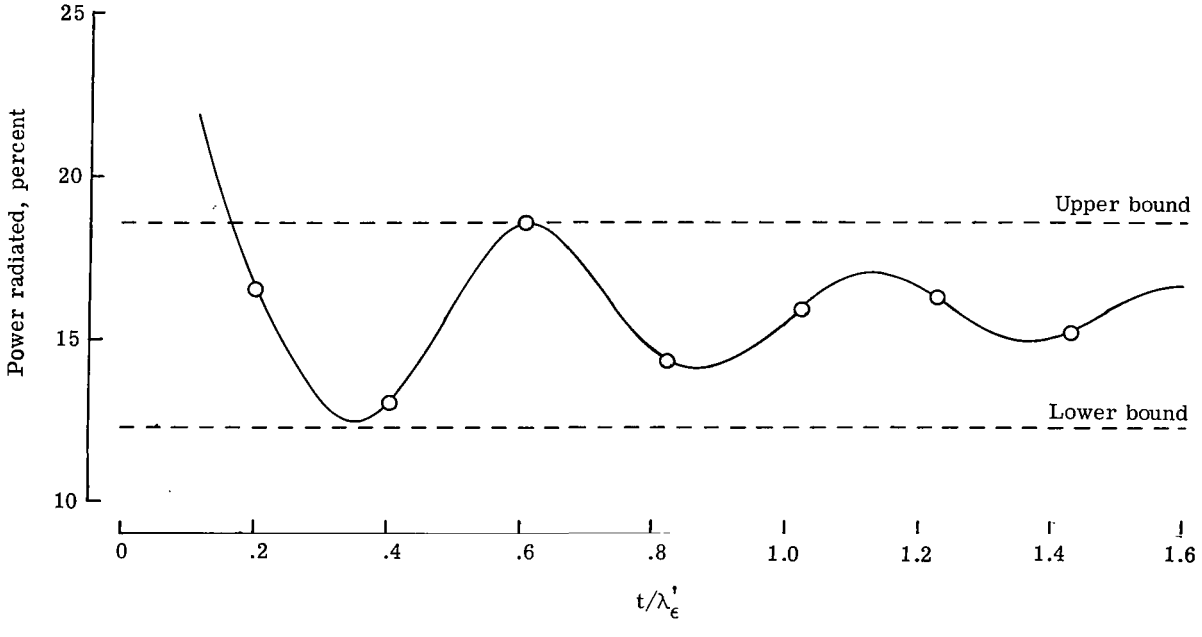

(b) f_r = 9.90 Gc/sec; l = 0.45 inch (1.143 cm); x_1 = 0.203 inch (0.516 cm).

Figure 18.- Measured power radiated by a cross slot at average resonant frequency as a function of cover thickness. ϵ = 3.76.

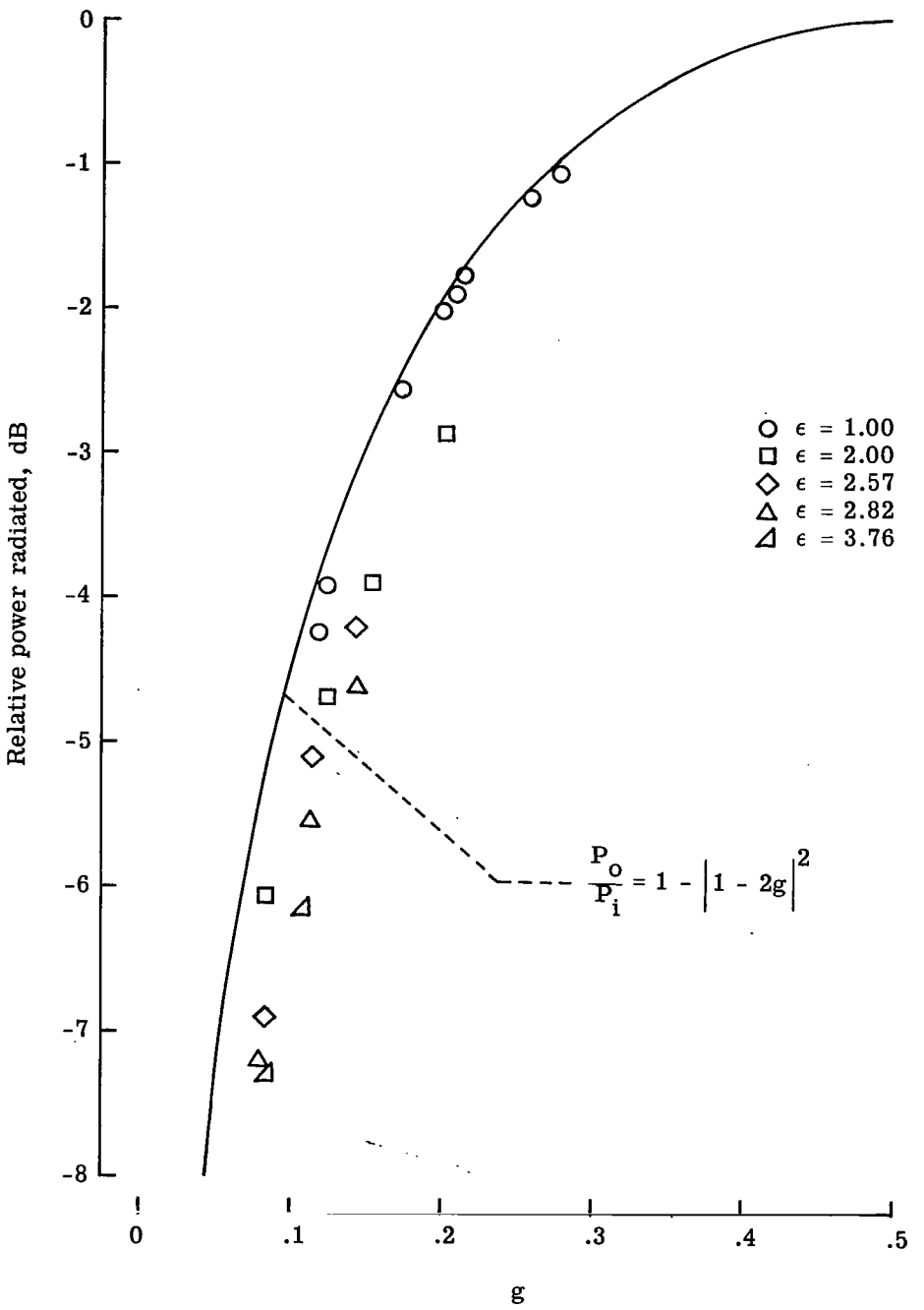

Figure 19.- Comparison of theory for semi-infinite medium with measured power radiated by cross slot under a finite dielectric slab of thickness approximately $0.6\lambda_\epsilon'$.

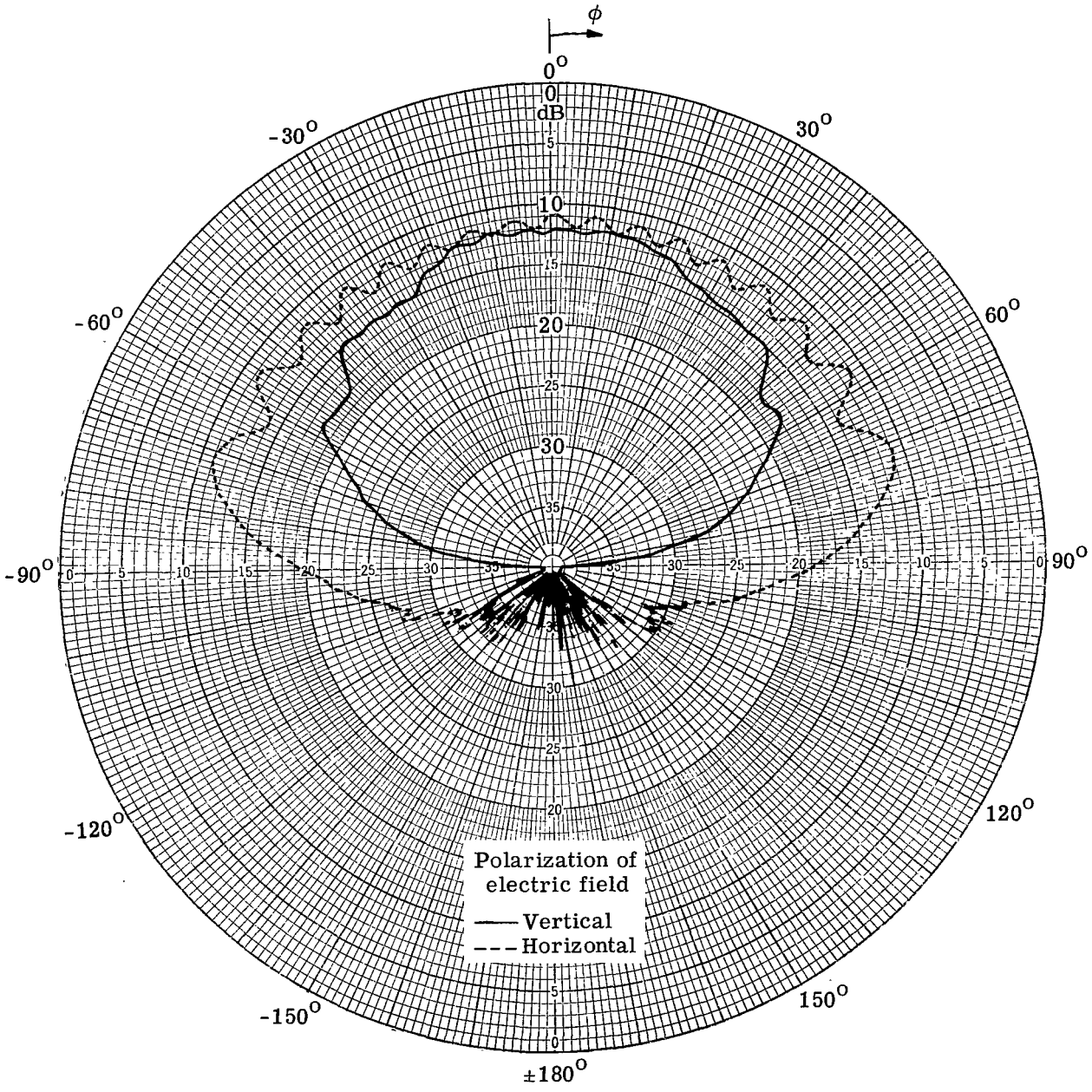

Figure 20.- Measured far-field power radiation patterns of a cross slot with no dielectric cover. l = 0.55 inch (1.397 cm); x_1 = 0.237 inch (0.602 cm); f = 8.9 Gc/sec.

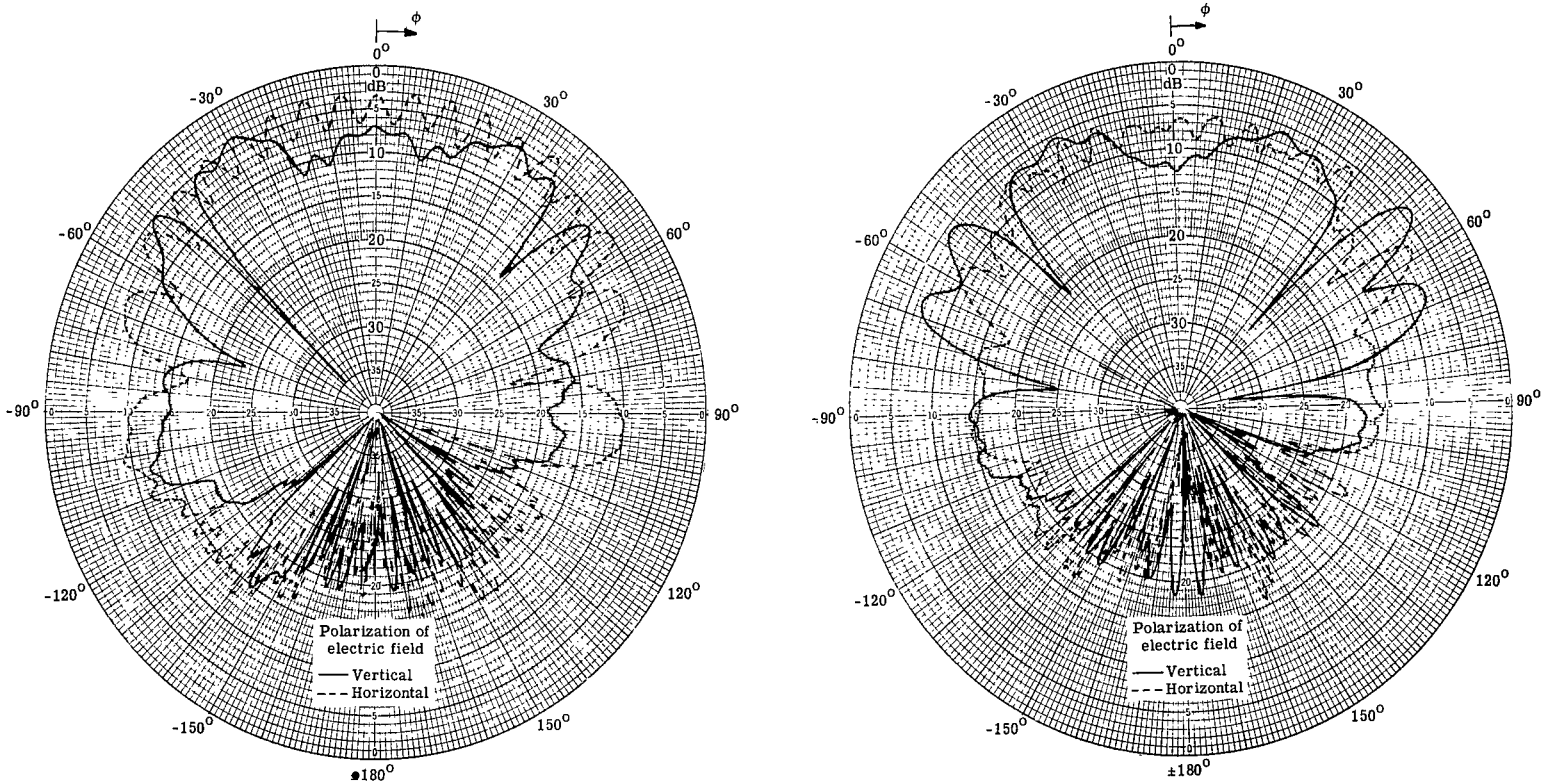

(a) t = 0.137 inch (0.348 cm); t/λ_ε = 0.166.

(b) t = 0.247 inch (0.627 cm); t/λ_ε = 0.298.

Figure 21.- Measured far-field power radiation patterns of a cross slot for several cover thicknesses. ε = 2.57; l = 0.55 inch (1.397 cm); x_1 = 0.237 inch (0.602 cm); f = 8.9 Gc/sec.

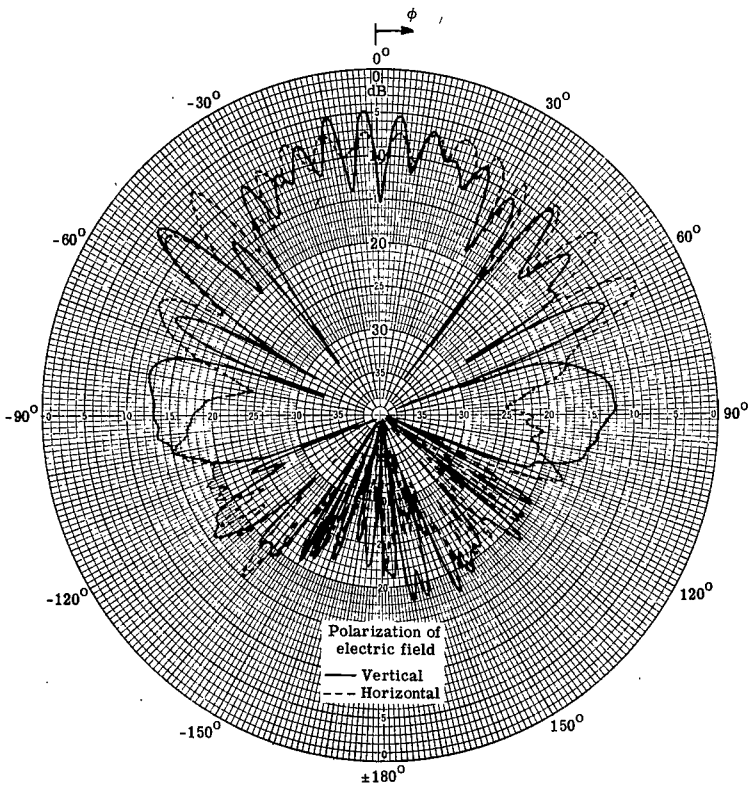

(c) t = 0.388 inch (0.986 cm); t/λ_ε = 0.469.

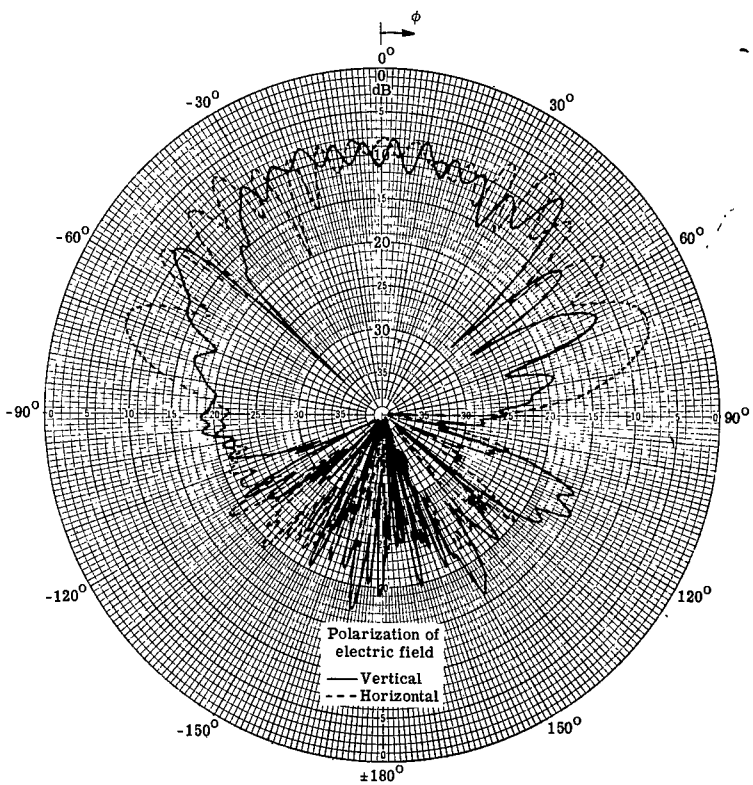

(d) t = 0.487 inch (1.237 cm); t/λ_ε = 0.588.

Figure 21.- Continued.

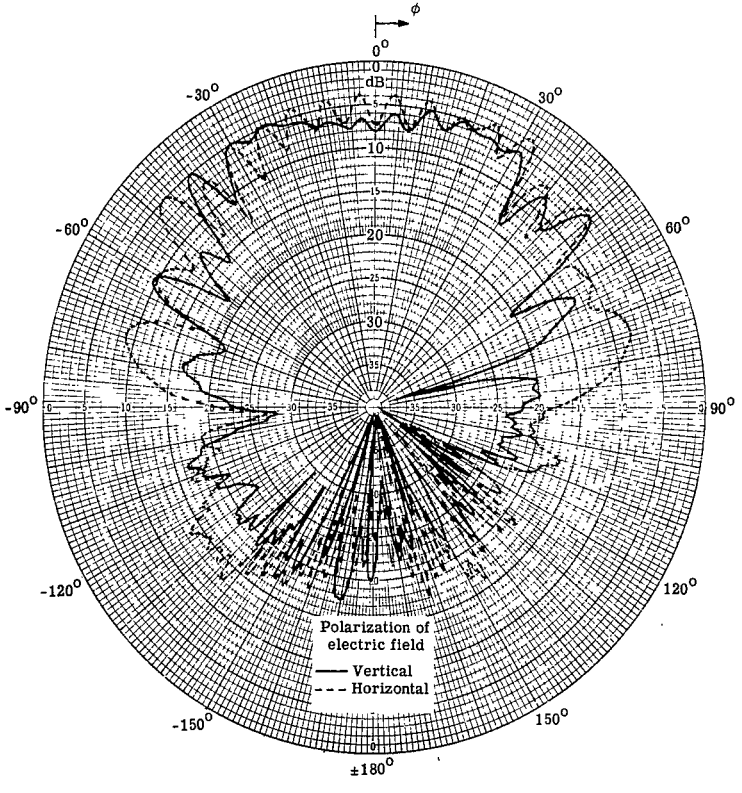

(e) t = 0.624 inch (1.585 cm); $t/\lambda_\varepsilon = 0.754$.

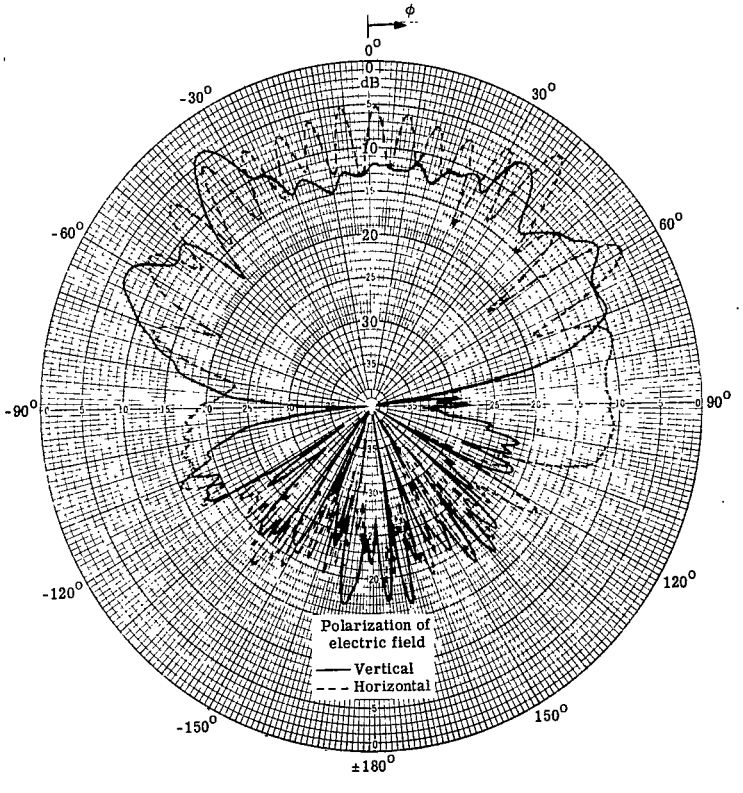

(f) t = 0.734 inch (1.864 cm); $t/\lambda_\varepsilon = 0.887$.

Figure 21.- Concluded.

"The aeronautical and space activities of the United States shall be conducted so as to contribute . . . to the expansion of human knowledge of phenomena in the atmosphere and space. The Administration shall provide for the widest practicable and appropriate dissemination of information concerning its activities and the results thereof."

—NATIONAL AERONAUTICS AND SPACE ACT OF 1958

NASA SCIENTIFIC AND TECHNICAL PUBLICATIONS

TECHNICAL REPORTS: Scientific and technical information considered important, complete, and a lasting contribution to existing knowledge.

TECHNICAL NOTES: Information less broad in scope but nevertheless of importance as a contribution to existing knowledge.

TECHNICAL MEMORANDUMS: Information receiving limited distribution because of preliminary data, security classification, or other reasons.

CONTRACTOR REPORTS: Scientific and technical information generated under a NASA contract or grant and considered an important contribution to existing knowledge.

TECHNICAL TRANSLATIONS: Information published in a foreign language considered to merit NASA distribution in English.

SPECIAL PUBLICATIONS: Information derived from or of value to NASA activities. Publications include conference proceedings, monographs, data compilations, handbooks, sourcebooks, and special bibliographies.

TECHNOLOGY UTILIZATION PUBLICATIONS: Information on technology used by NASA that may be of particular interest in commercial and other non-aerospace applications. Publications include Tech Briefs, Technology Utilization Reports and Notes, and Technology Surveys.

Details on the availability of these publications may be obtained from:

SCIENTIFIC AND TECHNICAL INFORMATION DIVISION

NATIONAL AERONAUTICS AND SPACE ADMINISTRATION

Washington, D.C. 20546